能となることが報告された。岩本朋忠氏（神戸市環境保健研究所）からは，地域分離株のVNTRデータに基づく遺伝子型別データベースの構築とその活用法について概説いただいた。VNTR法の特徴を生かして，結核対策プログラム上ハイリスクと考えられる株の出現を常時モニタリングする結核危機管理体制の整備ならびに海外分離結核菌との比較から得られた神戸市分離結核菌の特徴について報告された。

1. 沖縄県での長期にわたるRFLP分析の成果と課題

結核予防会結核研究所抗酸菌レファレンスセンター結核菌情報科　前田　伸司

はじめに

1996年から結核研究所と沖縄県福祉保健部は共同で，沖縄県内の保健所・医療機関等の協力のもと，新規登録結核患者で培養陽性例の約7割の株について挿入配列（IS）*6110*プローブを用いた制限酵素断片長多型（RFLP）分析を行ってきた[1)2)]。本研究プロジェクトは，通常の接触者調査だけではなく，分離された菌体から得られる分子疫学的情報を提供することにより，①患者発生調査の改善を計ることができる，②結核対策方針策定のための疫学情報を提供することができる，③将来全国的な結核菌DNA情報サーベイランスを導入する際の基礎となる知見が得られる，など接触者調査の改善と将来の大規模な結核菌DNA情報のデータベース化を目指したものである。

RFLP分析

沖縄県の現在の人口は約136万人（平成17年国勢調査速報）で，結核新規登録患者の推移をみると，1996年に年間400人を超えていたが，2004年は339人となり，年ごとに若干の変動はあるものの減少傾向にある。また，罹患率は全国平均，沖縄県共にほぼ同じ罹患率をたどって低下している。沖縄県での調査は，他県と隣接しない島であるという地域的な特徴があり，患者の移動も把握しやすいという利点がある。

分析を行った株は，1996年4月から2005年12月までの新規登録患者で塗抹検査または培養検査陽性となった結核菌1924株のうち，1323株（68.8%）であった。分析方法は，結核菌タイピングの標準法であるIS*6110*-RFLP分析を用いた[3)]。IS*6110*-RFLPは，結核菌ゲノム上にランダムに存在するトランスポゾンの配列の一部であるIS*6110*配列をサザンハイブリダイゼーション法で検出するというものである。分析で得られたバンド数は，ゲノム上に存在していたIS*6110*配列の数を反映し，位置（分子量）の違いは制限酵素サイトからIS*6110*配列までの距離を反映している。このようにRFLP分析では，挿入配列の数と酵素サイトからの距離という2つの独立した事象を利用して結核菌のタイピングを行うという手法である。集団発生例などで同一感染源から感染した患者から分離した菌は，同一のRFLPパターンを示し，逆にRFLP分析結果が同一パターンであれば，同一感染源から感染した結核である可能性が強く疑われることになる。実際の分析では，アガロースゲルの濃度，泳動時間などの条件等が異なる場合もあるため，それらを補正するためにコンピューター上でプログラムソフト（BioNumerics ver. 4.0, Applied Maths社）を使って解析を行った。分子量マーカーを使って各レーンの泳動距離を修正後，系統樹を作製して同一菌株，つまりクラスターを形成する株どうしを見つけ出し，分類を行った。

クラスター率

1323株を分析した結果，158種類のクラスターが存在することがわかった。最も多いのは，2株で構成されるクラスターで87種類存在し，最大クラスターはクラスター番号65で22株から構成されていた（Table）。分析した株の中で574株が何らかのクラスターを形成しており，クラスター率は43.4%（574/1323）であった。先進国の大都市では患者菌株の28～72%がクラスターを形成しているという報告[4)]があることから，このクラスター率は中程度の値であると考えられる。

各年齢階層別にクラスター率（折れ線グラフ）と実際に分析した株数（棒グラフ）の関係を表すと，若年齢層では分析した株数が少ないが，クラスター率が高い傾向がみられた（Fig. 1）。一方，高年齢層では，クラスター率が低くなるという傾向がみられた。しかし，これらの違いは，統計学的に有意な差ではなかった。一般的にクラスター率が高いということは，最近の感染を反映しているといわれている。つまり，若年層ではクラスター率が高く，高年齢層では加齢によって細胞性免疫の低下が起こり内因性再燃の頻度が高くなることからクラスター率が低くなるという報告[5)]と今回の結果は，一致するものだった。

Table Cluster code and number of strains

Cluster code	No. of strains	Cluster code	No. of strains	Cluster code	No. of strains	Cluster code	No. of strains	Cluster code	No. of strains
3a	5	43T	3	73da	4	84	7	126	20
8	4	46	12	73f	3	85	10	126e	4
8a	3	48	7	73h	4	85a	7	128	4
8aa	14	50	10	73k	4	85aa	3	131	12
9b	5	50aa	3	73o	5	94	3	142	3
10a	3	52	3	75	3	108	7	151	3
12	6	52b	3	77	3	108a	5	157	4
18	5	55a	3	78	3	110	3	167	3
20	3	63	3	79	3	111	3	169	4
24	17	65	22	79a	5	112a	7	170	3
27	3	66	3	80	4	116	5	173	3
27a	3	67	3	80a	4	118	3		
32	4	73	20	80aa	6	121	5		
33	9	73a	3	80aT	4	122	6		
33e	4	73d	13	82	5	123	4		

Except for the clusters which consist of 2 strains, the clusters composed of three or more strains were shown in this table.

成果と問題点

クラスター番号65番の株を分析することによって，八重山における地域内流行型結核菌の存在を示唆する結果が得られている（Fig. 2）。これは1996年から2003年までの8年間にわたって散発的に22例ほど検出された結核菌で，疫学的調査にもかかわらず，ほとんどの例で関連が不明であった。年齢分布は，70歳で過去結核既往歴のある老人から10歳の小児まで広い範囲に及んでいた。唯一，疫学的関係が明らかになったのは，家族内での感染例である3例のみであった。すべての患者で共通する点としては，患者が石垣市在住か，あるいは過去に八重山に滞在したことがあるということであった。つまり，この結核菌は過去に八重山地区内で流行してい

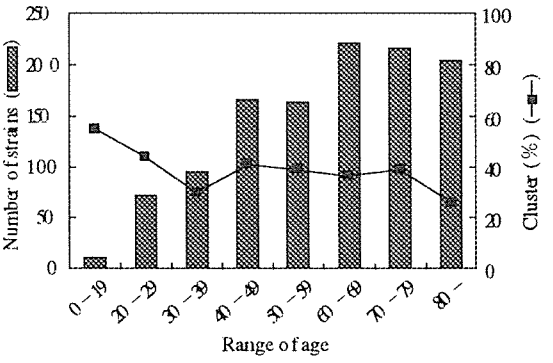

Fig. 1 Number of analyzed strains and percentage of clustered cases by age group

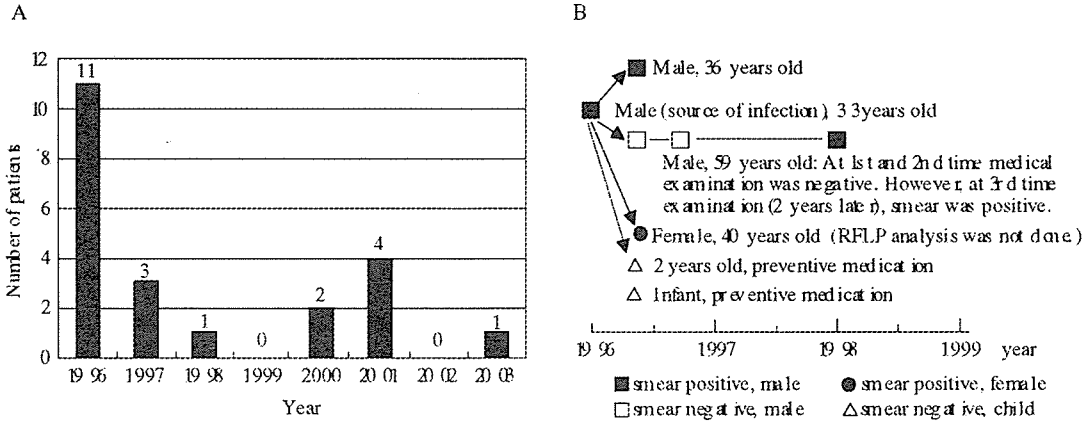

Fig. 2 Presumed route of TB infection in cluster code 65. (Possibility of existing the endemic type of *M. tuberculosis*) Number of patients infected with the code 65 strain (A). The only example that epidemiologic connection became clear was family infection case (B).

た地域性の高い流行株であることが示唆された。このような結核菌存在の証明は，沖縄県で長期にわたって結核菌を分析することによって明らかになったものであり，本研究プロジェクトの大きな成果である。

しかしながら，分子疫学を利用したRFLP分析結果から得られたクラスターのうちで，疫学的検討により伝播が証明できたのは，全体の約10%以下であり非常に低いものだった。このようにRFLP分析の結果が，実際の接触者調査の場で十分に活用されていないという現状である。この原因としては，①分析には1μg以上の精製した高分子DNAが必要で，菌の培養が必要で時間がかかる。そのため，結核患者登録とRFLP分析結果の報告とに時間的なギャップを生じて，再調査において患者との再面接等有意義な情報収集が困難である，②RFLP分析を実施する場合，生きた菌を検査施設に送らなければならず，かなりの手間がかかる，ということが考えられる。

また，RFLP分析結果は画像データとして得られるので，多施設間での結果の比較は全く同じ方法・装置によらなければ困難であるというRFLP分析法自体の欠点がある。

分子疫学の今後

分子疫学の成果を結核対策に生かすためには，接触者調査等を有効に行うことができるように，結果報告の迅速化が第一である。このためには，菌の輸送法の検討や分析法を含めた検討が必要となると考えられる。特に大都市周辺では，行政区域を越えて人が移動することが日常となっていることから，保健所の管轄を越えても追跡調査が可能な統一した方法で分子疫学調査を進める必要がある。このような要求に合致した方法のひとつとして，反復配列多型（Variable Numbers of Tandem Repeats: VNTR）分析法がある[6]。

結核研究所では，このVNTR法が現在の標準法であるRFLP分析に代わる方法と成りえるのかどうかの検討を行っている。現状のVNTR分析の標準となる12カ所のMycobacterial Interspersed Repetitive Unit（MIRU）と4カ所のExact Tandem Repeat（ETR）について253株の結核菌を分析した。その結果，30種類のクラスターが観察され，最大のクラスターサイズは42株からなるクラスターだった。VNTR分析によるクラスター率は62.8%で，同じ菌株を用いたRFLP分析でのクラスター率が29.6%だったことから，クラスター率を指標に判断すると，16カ所のVNTR分析法は，RFLP分析に比べてタイピング能力が著しく低いことがわかった。そのため，この方法をそのままRFLP分析法に代えて結核菌のタイピング法として利用できないことが明らかになった。

個々のlocusについて検討を行うと，例えばMIRU26のようにバリエーションの高い部位，逆にMIRU2，MIRU24のように低い部位が存在していることがわかった。そのため，現在の標準と考えられている分析部位以外で多型性の高い新しいVNTR部位を探し，RFLP分析法と同等のタイピング能力を得るには，どのlocusの組み合わせが適当であるのか検討を行っている。

北京型結核菌が多くの割合を占める日本国内の結核菌を分析するための最適なVNTR法の確立が急務である。そして，適切なlocusを選択し，適切なlocus数を分析すれば，現在の標準法であるIS*6110*-RFLP分析と同程度の分解能をもったVNTR分析法の確立が可能であると考えられる。

ま と め

沖縄県で長期にわたって行ってきた結核菌のRFLP分析により，地域流行型結核菌が存在することを明らかにすることができた。また，より有効な接触者調査のために，分子疫学による結核菌情報を積極的に利用できるようにすることが必要である。そのためには，まず分析結果報告の迅速化が必要な対策であり，日本における標準的VNTR法の確立を行い，RFLP分析法から遺伝子増幅法を利用するVNTR法にシフトしていく必要がある。

謝 辞

本研究は，結核予防会結核研究所研究部分子疫学プロジェクト研究の一環として行われてきたものであり，その構成員の皆様に感謝致します。特に国内においてRFLP分析法の有効性を広めた高橋光良先生に深く感謝致します。

文 献

1）沖縄県結核サーベイランス検討委員会：沖縄県の結核患者管理における結核菌遺伝子型同定の有用性．日本公衆衛生雑誌．2003；50：339-348.
2）大角晃弘，高橋光良，内村和宏，他：結核菌DNA指紋法を用いた結核対策改善事業成績（1996年4月～2004年5月の概略）．資料と展望．2004; 51: 77-83.
3）van Embden JD, Cave MD, Crawford JT, et al.: Strain identification of *Mycobacterium tuberculosis* by DNA fingerprinting: recommendations for a standardized methodology. J Clin Microbiol. 1993；31：406-409.
4）森 亨：地域分子疫学の結核対策への応用．資料と展望．2004；51：45-57.
5）阿野裕美，松本智成，吉多仁子，他：IS*6110* RFLP解析に基づく，結核の分子疫学的検討―2001年～2003年―．結核．2006；81：321-328.
6）Supply P, Mazars E, Lesjean S, et al.: Variable human minisatellite-like regions in the *Mycobacterium tuberculosis* genome. Mol Microbiol. 2000；36：762-771.

JOURNAL OF CLINICAL MICROBIOLOGY, Jan. 2007, p. 179–192 Vol. 45, No. 1
0095-1137/07/$08.00+0 doi:10.1128/JCM.00750-06

Detection of Multidrug Resistance in *Mycobacterium tuberculosis*▽

Jun-ichiro Sekiguchi,[1] Tohru Miyoshi-Akiyama,[1] Ewa Augustynowicz-Kopeć,[2] Zofia Zwolska,[2] Fumiko Kirikae,[1] Emiko Toyota,[1] Intetsu Kobayashi,[3] Koji Morita,[4] Koichiro Kudo,[1] Seiya Kato,[5] Tadatoshi Kuratsuji,[1,6] Toru Mori,[5,7] and Teruo Kirikae[1]*

International Medical Center of Japan, 1-21-1 Toyama, Shinjuku, Tokyo 162-8655, Japan[1]; National Research Institute of Tuberculosis and Lung Diseases, Plocka St. 26, Warsaw 01-138, Poland[2]; Mitsubishi Kagaku Bio-Clinical Laboratories, Inc., 3-30-1 Shimura, Itabashi, Tokyo174-8555, Japan[3]; Department of Microbiology, Kyorin University School of Health Sciences, 476 Miyashita, Hachioji, Tokyo 192-8508, Japan[4]; Research Institute of Tuberculosis, Japan Anti-Tuberculosis Association, Matsuyama 3-1-24, Kiyose, Tokyo 204-8533, Japan[5]; National Research Institute for Child Health and Development, Setagaya, Tokyo 157-8535, Japan[6]; and Leprosy Research Center, National Institute of Infectious Diseases, 4-2-1 Aoba-cho, Higashimurayama, Tokyo 189-0002, Japan[7]

Received 8 April 2006/Returned for modification 3 July 2006/Accepted 9 October 2006

We developed a DNA sequencing-based method to detect mutations in the genome of drug-resistant *Mycobacterium tuberculosis*. Drug resistance in *M. tuberculosis* is caused by mutations in restricted regions of the genome. Eight genome regions associated with drug resistance, including *rpoB* for rifampin (RIF), *katG* and the *mabA* (*fabG1*)-*inhA* promoter for isoniazid (INH), *embB* for ethambutol (EMB), *pncA* for pyrazinamide (PZA), *rpsL* and *rrs* for streptomycin (STR), and *gyrA* for levofloxacin, were amplified simultaneously by PCR, and the DNA sequences were determined. It took 6.5 h to complete all procedures. Among the 138 clinical isolates tested, 55 were resistant to at least one drug. Thirty-four of 38 INH-resistant isolates (89.5%), 28 of 28 RIF-resistant isolates (100%), 15 of 18 EMB-resistant isolates (83.3%), 18 of 30 STR-resistant isolates (60%), and 17 of 17 PZA-resistant isolates (100%) had mutations related to specific drug resistance. Eighteen of these mutations had not been reported previously. These novel mutations include one in *rpoB*, eight in *katG*, one in the *mabA-inhA* regulatory region, two in *embB*, five in *pncA*, and one in *rrs*. *Escherichia coli* isolates expressing individually five of the eight *katG* mutations showed loss of catalase and INH oxidation activities, and isolates carrying any of the five *pncA* mutations showed no pyrazinamidase activity, indicating that these mutations are associated with INH and PZA resistance, respectively. Our sequencing-based method was also useful for testing sputa from tuberculosis patients and for screening of mutations in *Mycobacterium bovis*. In conclusion, our new method is useful for rapid detection of multiple-drug-resistant *M. tuberculosis* and for identifying novel mutations in drug-resistant *M. tuberculosis*.

The emergence and spread of drug-resistant strains of *Mycobacterium tuberculosis*, especially multidrug-resistant (MDR) strains, are serious threats to the control of tuberculosis and comprise an increasing public health problem (40). Patients infected with MDR strains, which are defined as strains resistant to both rifampin (RIF) and isoniazid (INH), are difficult to cure and are more likely to remain sources of infection for a longer period of time than are patients with drug-susceptible strains (40).

It is essential that rapid drug susceptibility tests be developed to prevent the spread of MDR *M. tuberculosis*. The time necessary for culture of specimens was reduced by the radiometric BACTEC 460TB system (BD Biosciences, Sparks, MD), the nonradiometric ESP II system (Trek Diagnostics, Westlake, OH), and other rapid broth methods, such as BACTEC MGIT 960 SIRE (BD Biosciences) (20). These drug susceptibility tests, however, still require 1 to 2 weeks for final determination and reporting to the clinician (23). Additional reductions in the detection period are needed.

* Corresponding author. Mailing address: Department of Infectious Diseases, Research Institute, International Medical Center of Japan, 1-21-1 Toyama, Shinjuku, Tokyo 162-8655, Japan. Phone: (81) 3 3202 7181, ext. 2838. Fax: (81) 3 3202 7364. E-mail: tkirikae@ri.imcj.go.jp.

▽ Published ahead of print on 15 November 2006.

Drug resistance in *M. tuberculosis* is caused by mutations in relatively restricted regions of the genome (17, 39). Mutations associated with drug resistance occur in *rpoB* for RIF, *katG* and the promoter region of the *mabA* (*fabG1*)-*inhA* operon for INH, *embB* for ethambutol (EMB), *pncA* for pyrazinamide (PZA), *rpsL* and *rrs* for streptomycin (STR), and *gyrA* for fluoroquinolones (FQs) such as ofloxacin (OFX) and levofloxacin (LVX) (17, 39). For example, 96% to 100% of RIF-resistant *M. tuberculosis* isolates have at least 1 mutation in *rpoB*, which encodes the RNA polymerase β-subunit (17, 31, 39). Of INH-resistant isolates, 42% to 58% have at least 1 mutation in *katG*, which encodes catalase-peroxidase, and 21% to 34% carry at least 1 mutation in the promoter of *mabA*, a synonym for *fabG1* (10), which encodes a 3-ketoacyl reductase (3, 17, 38, 39). Of EMB-resistant isolates, 47% to 65% have at least one mutation in *embB*, which encodes arabinosyltransferase (17, 32, 39). Seventy-two to 97% of PZA-resistant isolates have at least one mutation in *pncA*, which encodes pyrazinamidase (17, 26, 39). Of STR-resistant isolates, 52% to 59% and 8% to 21% have mutations in *rpsL*, which encodes ribosomal protein S12, and *rrs*, which encodes 16S rRNA, respectively (17, 19, 39). Of FQ-resistant isolates, 75% to 94% have mutations in *gyrA*, which encodes the A subunit of DNA gyrase (17, 30, 39).

Various molecular methods have been used to identify the

TABLE 1. Bacterial strains used in the present study

Strain	Characteristic(s) or susceptibility pattern	No. of isolates
M. tuberculosis IMCJ	Clinical strains isolated in Japan	105
	Rif^r Inh^r Emb^r Pza^r Str^r Ofx^r	3
	Rif^r Inh^r Emb^r Pza^r Str^r	3
	Rif^r Inh^r Pza^r Str^r	3
	Rif^r Inh^r Emb^r Str^r	4
	Rif^r Inh^r Emb^r Pza^r	2
	Inh^r Emb^r Str^r	2
	Rif^r Inh^r	2
	Inh^r Str^r	4
	Pza^r Str^r	1
	Rif^r Str^r	2
	Rif^r	2
	Inh^r	5
	Pza^r	2
	Str^r	6
	Susceptible to all drugs tested	64
M. tuberculosis P	Clinical strains isolated in Poland	33
	Rif^r Inh^r Emb^r Pza^r	1
	Rif^r Inh^r Emb^r	2
	Rif^r Inh^r Pza^r	1
	Rif^r Inh^r	2
	Inh^r Str^r	1
	Rif^r	1
	Inh^r	3
	Emb^r	1
	Pza^r	1
	Str^r	1
	Susceptible to all drugs tested	19
M. tuberculosis H37Rv (ATCC[a] 27294)	Susceptible to all drugs tested	1
M. tuberculosis H37Ra (ATCC 25177)	Susceptible to all drugs tested	1
M. avium ATCC 25291	ND[g]	1
M. bovis BCG[b] (Japanese strain 172)	Pza^r	1
M. chelonae JCM[c] 6390 (ATCC 14472)	ND	1
M. fortuitum RIMD[d] 1317004 (ATCC 6841)	ND	1
M. gastri GTC[e] 610 (ATCC 15754)	ND	1
M. intracellulare JCM 6384 (ATCC 13950)	ND	1
M. kansasii JCM 6379 (ATCC 124878)	ND	1
M. marinum GTC 616 (ATCC 927)	ND	1
M. nonchromogenicum JCM 6364 (ATCC 19530)	ND	1
M. phlei RIMD 1326001 (ATCC19249)	ND	1
M. scrofulaceum JCM 6381 (ATCC 19981)	ND	1
M. simiae GTC 620 (ATCC 25275)	ND	1
M. smegmatis ATCC 19420	ND	1
M. szulgai JCM 6383 (ATCC 35799)	ND	1
M. terrae GTC 623 (ATCC 15755)	ND	1
Escherichia coli ATCC 8739	ND	1
Haemophilis influenzae IID[f] 984 (ATCC 9334)	ND	1
Klebsiella pneumoniae IID5209 (ATCC 15380)	ND	1
Legionella pneumophila GTC 745	ND	1
Mycoplasma pneumoniae IID 817	ND	1
Pseudomonas aeruginosa ATCC 27853	ND	1
Rhodococcus equi ATCC 33710	ND	1
Staphylococcus aureus N315	ND	1
Streptococcus pneumoniae GTC 261	ND	1

[a] American Type Culture Collection, Rockville, MD.
[b] Japan BCG Laboratory, Tokyo, Japan.
[c] Japan Collection of Microorganisms, Institute of Physical and Chemical Research (RIKEN), Saitama, Japan.
[d] Research Institute for Microbial Diseases, Osaka University, Osaka, Japan.
[e] Gifu Type Culture Collection, Department of Microbiology-Bioinformatics, Regeneration and Advanced Medical Science, Gifu University, Graduate School of Medicine, Bacterial Genetic Resources, Gifu, Japan.
[f] Institute of Medical Science, University of Tokyo, Tokyo, Japan.
[g] ND, not determined.

mutations in *rpoB*, *katG*, *rpsL*, *rrs*, *embB*, *pncA*, *gyrA*, and other genes (7, 17). Among these methods, DNA sequencing is the most direct and reliable for detection of both known and novel mutations. The conventional methods, nevertheless, are not applicable for analysis of strains that may have multiple mutations in genes related to drug resistance because different PCR conditions are required for amplification of each target region. We describe here a new PCR-based method for simultaneous detection of mutations in eight genes responsible for resistance to six antitubercular drugs.

MATERIALS AND METHODS

Bacterial strains and plasmids. One hundred five and 33 clinical isolates of *M. tuberculosis* were obtained from patients with pulmonary tuberculosis in Japan and Poland, respectively. All of the bacterial strains used in this study, except for those used in cloning experiments, are listed in Table 1. *Escherichia coli* UM262 (*recA katG*::Tn*10 pro leu rpsL hsdM hsdR endl lacY*) (13) was provided by Barbara L. Triggs-Raine (University of Manitoba, Manitoba, Canada) and was used as a host for the expression of *katG* derived from *M. tuberculosis* clinical isolates and H37Rv, an *M. tuberculosis* reference strain. *E. coli* TOP10 (Invitrogen, Carlsbad, CA) and BL21-AI (Invitrogen) were used as hosts for cloning and protein overexpression studies, respectively. pCRT7/NT (Invitrogen) was used as a cloning and protein expression vector.

Drug susceptibility test. All clinical isolates of *M. tuberculosis*, *M. tuberculosis* strains H37Rv and H37Ra, and *Mycobacterium bovis* BCG Japanese strain 172 were tested for drug susceptibility. Strains were analyzed by three different methods. Two methods were agar proportion methods: the Middlebrook 7H10 agar medium method recommended by the United States Public Health Service (20) and the egg-based Ogawa medium method recommended by the Japanese Society for Tuberculosis (Vit Spectrum-SR; Kyokuto Pharmaceutical Industrial Co., Tokyo, Japan). The third method was a rapid broth method (BD BACTEC MGIT 960 SIRE, BD Biosciences, Sparks, MD) (20). The proportion method with 7H10 agar medium was used to assess susceptibilities to RIF, INH, EMB, STR, and OFX. Ogawa medium was used to test susceptibilities to RIF, INH, EMB, SM, and LVX. The broth method was applied to assess susceptibilities to RIF, INH, EMB, STR, and PZA. All isolates were tested by all three methods.

Assay for PZase activity. Pyrazinamidase (PZase) activity was determined as described previously (34). *M. tuberculosis* strain H37Rv, which is susceptible to PZA and positive for PZase, was used as a positive control for the assay. *M. bovis* strain BCG, which is resistant to PZA and negative for PZase, was used as a negative control. Each test tube was read and classified by three independent observers. There were no discrepancies between the classifications for any of the isolates tested.

DNA extraction. Genomic DNAs from bacteria were extracted as described previously (21).

Clinical samples. Six samples of mycobacterial staining-positive sputa from six patients with relapsed active tuberculosis and four samples of staining-negative sputa from four patients who had been treated previously with antitubercular drugs, were treated with *N*-acetyl-L-cysteine–NaOH solution according to the procedure of the BBL MycoPrep mycobacterial system digestion/decontamination kit (BD Diagnostic Systems, Franklin Lakes, NJ). Each sample was resuspended in 1.5 ml phosphate buffer. One milliliter of the suspension was transferred to a 1.5-ml tube for PCR. The remaining suspension was inoculated into Ogawa medium and MGIT 960 broth and cultured for mycobacterial examination. The 1 ml of suspension for PCR was centrifuged for 15 min at 13,000 × *g*, and the supernatant was removed with a pipette. Tris-EDTA (TE) buffer (500 μl) was added to resuspend the sediment, and the solution was again centrifuged for 15 min at 13,000 × *g*. The sediment was resuspended in 100 μl of a 10% solution of Chelex 100 resin (Bio-Rad Laboratories, Hercules, CA) in distilled water. The sample was resuspended by vortexing and incubated at 45°C for 45 min followed by incubation at 100°C for 10 min. The sample was vortexed again, allowed to cool, and centrifuged at 12,000 × *g* for 5 min to clarify the supernatant, which was transferred to another 1.5-ml tube and used for PCR.

DNA sequencing of drug resistance-related genes. Eight pairs of PCR primers were designed to amplify simultaneously regions of eight genes associated with resistance to six antituberculosis drugs. Sixteen primers were designed to determine the DNA sequences of the amplicons. The sequences of oligonucleotide primers for PCR, PR1 to PR16, and for DNA sequencing, PR17 to PR32, and the regions analyzed are listed in Table 2.

A two-temperature PCR consisting of 30 cycles of 95°C for 1 s for denaturation and 68°C for 30 s for annealing and elongation was performed with a GeneAmp PCR system 9700 thermocycler (Applied Biosystems, Foster City, CA) for DNA amplification, according to the instructions in the manufacturer's manual. Each PCR primer pair in TE (1.0 μl of 10 μM) listed in Table 2 was added to an individual reaction tube (0.2 ml Thermo-Tube; Advanced Biotechnologies, Epsom, Surrey, United Kingdom). Hence, eight reaction tubes containing the different primer pairs were prepared. Forty-nine microliters of a solution containing 1.0 μl DNA template, 1.25 U *Z-Taq* polymerase (Takara Bio, Ohtsu, Shiga, Japan), 4 μl of 2.5 mM each deoxynucleotide triphosphate, and 5 μl of 10× Z *Taq* PCR buffer (Takara Bio) was added to each reaction tube. The *Z-Taq* polymerase offers unmatched PCR productivity, with a processing speed five times faster than those of other commercially available *Taq* polymerases, which allowed us to reduce the annealing and elongation times.

PCR products were purified with MicroSpin S-300 HR columns (Amersham Biosciences, Uppsala, Sweden) or a DyeEx 2.0 spin kit (QIAGEN K.K., Tokyo, Japan) and used as templates for DNA sequencing. PCR products were sequenced with the appropriate gene-specific primers (Table 2). Sequencing was performed with an ABI PRISM BigDye terminator cycle sequencing ready reaction kit for a 96-well format (Applied Biosystems). Five microliters of premixed reagents from the kit (Terminator Ready Reaction mix; Applied Biosystems) and 13.5 μl of 1× reaction buffer were added to each tube containing 100 ng of templates and 5 pmol sequencing primer and mixed with a pipette. Amplification conditions were 25 cycles of 96°C for 10 s for denaturation, 50°C for 5 s for annealing, and 60°C for 4 min for elongation. It took 2.5 h to complete the entire reaction. Centri-Sep spin columns (Applied Biosystems) were used to remove unincorporated reagents and primers. Purified products were dried in a vacuum centrifuge, resuspended in Hi-Di formamide (Applied Biosystems), heated for 2 min at 95°C for denaturation, immediately cooled on ice, and loaded into a 96-well plate (MicroAmp 96-well reaction plate; Applied Biosystems). The purified samples were then analyzed with an ABI PRISM 3100 genetic analyzer (Applied Biosystems). DNA sequences were collected and edited with Data Collection version 1.01 and Sequencing Analysis version 3.7 software (Applied Biosystems) and compared with those of *M. tuberculosis* H37Rv (GenBank accession no. NC_000962) with Genetyx-WIN (version 5; Software Development Co., Tokyo, Japan). The codon numbers of *rpoB* were designated on the basis of alignment of the *E. coli rpoB* sequence with a portion of the *M. tuberculosis* H37Rv sequence and are not the positions of the actual *M. tuberculosis rpoB* codons (14, 31).

Cloning of *katG*. The coding regions of *katG* from six INH-resistant clinical isolates of *M. tuberculosis*, two INH-susceptible isolates, and the H37Rv strain were cloned. *katG* was amplified by PCR with 2.5 U of Easy-A high-fidelity PCR cloning enzyme (Stratagene, La Jolla, CA) and primers PR3 and PR4 (Table 2). The PCR products were ligated into the pCRT7/NT vector downstream of the region encoding a His_6 tag.

KatG enzyme assays. For expression of *M. tuberculosis* KatG, *katG*-deficient *E. coli* UM262 (13) cells were transformed with pCRT7/NT carrying cloned *katG* genes derived from eight clinical isolates and the H37Rv strain. KatG-mediated catalase activity was assayed spectrophotometrically by monitoring the decrease in H_2O_2 concentration at A_{240} (ε_{240} = 0.0436 mM^{-1} cm^{-1}) as described previously (18).

Assay for free-radical formation from INH oxidation. Rates of KatG-mediated free-radical formation from INH oxidation in the presence of H_2O_2 were monitored spectrophotometrically by following the reduction of nitroblue tetrazolium (NBT) as described previously (35).

Purification of KatG. *M. tuberculosis* KatG from strain H37Rv was overexpressed in *E. coli* BL21-AI cells and purified with chelating Sepharose (Ni Sepharose 6 Fast Flow; Amersham Biosciences) loaded with Ni^{2+} in a column. The purity of the KatG protein was more than 95% by 10% sodium dodecyl sulfate-polyacrylamide gel electrophoresis.

Enzyme-linked immunosorbent assay and Western blotting. Purified His-tagged KatG was used as an antigen to raise polyclonal antibodies in a male Japanese white rabbit. Antiserum against KatG was used for Western blotting and enzyme-linked immunosorbent assay.

Data analysis. The correlations between mutation data from the DNA sequence-based assays and data from conventional culture methods with drugs or PZase activities were assessed by the index of test efficiency. The efficiency of a test was defined as the percentage of times that the test gave the correct answer compared to the total number of tests.

RESULTS

Drug susceptibility patterns. The susceptibility patterns of the 138 clinical isolates for six drugs, RIF, INH, EMB, PZA, STR, and OFX, are shown in Table 1. Among the 138 clinical isolates, 55 were resistant to at least one drug and 23 were MDR strains displaying resistance to both INH and RIF. Twenty of the 23 MDR strains were resistant to at least one other drug in addition to INH and RIF. Eighty-three clinical isolates and 2 laboratory strains, H37Rv and H37Ra, were susceptible to all of the drugs tested. The BCG strain

TABLE 2. Primers used to detect MDR tuberculosis

Target gene[a]	Primer set (direction)	Nucleotide sequence	Positions[b]	Product size (bp)
PCR primers				
rpoB	PR1 (forward)	5′-CCGCGATCAAGGAGTTCTTC-3′	1256–1275	315
	PR2 (reverse)	5′-ACACGATCTCGTCGCTAACC-3′	1570–1551	
katG	PR3 (forward)	5′-GTGCCCGAGCAACACCCACCCATTACAGAAAC-3′	1–32	2,223
	PR4 (reverse)	5′-TCAGCGCACGTCGAACCTGTCGAG-3′	2223–2200	
mabA promoter	PR5 (forward)	5′-ACATACCTGCTGCGCAATTC-3′	−217 to −198	1,362
	PR6 (reverse)	5′-GCATACGAATACGCCGAGAT-3′	1145–1126	
embB	PR7 (forward)	5′-CCGACCACGCTGAAACTGCTGGCGAT-3′	640–665	2,748
	PR8 (reverse)	5′-GCCTGGTGCATACCGAGCAGCATAG-3′	3387–3303	
pncA	PR9 (forward)	5′-GGCGTCATGGACCCTATATC-3′	−80 to −61	670
	PR10 (reverse)	5′-CAACAGTTCATCCCGGTTC-3′	590–572	
rpsL	PR11 (forward)	5′-CCAACCATCCAGCAGCTGGT-3′	4–23	572
	PR12 (reverse)	5′-GTCGAGAGCCCGCTTGAGGG-3′	575–556	
rrs (16S RNA)	PR13 (forward)	5′-AAACCTCTTTCACCATCGAC-3′	428–447	1,329
	PR14 (reverse)	5′-GTATCCATTGATGCTCGCAA-3′	1756–1737	
gyrA	PR15 (forward)	5′-GATGACAGACACGACGTTGC-3′	−1–19	398
	PR16 (reverse)	5′-GGGCTTCGGTGTACCTCAT-3′	397–379	
Sequencing primers				
rpoB	PR17	5′-TACGGCGTTTCGATGAAC-3′ (complementary strand)	1529–1512	
katG	PR18	5′-ACGTAGATCAGCCCCATCTG-3′ (complementary strand)	689–670	
	PR19	5′-GAGCCCGATGAGGTCTATTG-3′	574–593	
	PR20	5′-CCGATCTATGAGCGGATCAC-3′	1162–1181	
	PR21	5′-GAACAAACCGACGTGGAATC-3′	1729–1748	
mabA promoter	PR22	5′-ACATACCTGCTGCGCAATTC-3′	−217 to −198	
embB	PR23	5′-ACGCTGAAACTGCTGGCGAT-3′	646–665	
	PR24	5′-GTCATCCTGACCGTGGTGTT-3′	1462–1481	
	PR25	5′-GGTGGGCAGGATGAGGTAGT-3′ (complementary strand)	1596–1577	
	PR26	5′-CACAATCTTTTTCGCCCTGT-3′	2007–2026	
	PR27	5′-GCGTGGTATCTCCTGCCTAAG-3′	2581–2601	
pncA	PR28	5′-GGCGTCATGGACCCTATATC-3′	−80 to −61	
rpsL	PR29	5′-CCAACCATCCAGCAGCTGGT-3′	4–23	
rrs (16S RNA)	PR30	5′-CAGGTAAGGTTCTTCGCGTTG-3′ (complementary strand)	979–959	
	PR31	5′-GTTCGGATCGGGGTCTGCAA-3′	1291–1310	
gyrA	PR32	5′-GATGACAGACACGACGTTGC-3′	−1–19	

[a] The complete sequences of target genes in *M. tuberculosis* H37Rv are in the GenBank database under accession no. NC_000962.
[b] Numbering based on nucleotide position relative to the initiation codon of each gene.

was sensitive to all drugs tested except PZA. When the results of the proportion method were compared with those of the Vit Spectrum-SR and BD BACTEC MGIT 960 SIRE methods, there was full agreement for all drugs. However, there were some differences in the degrees of susceptibility to INH between the methods. One hundred isolates were susceptible to 0.2 μg/ml of INH when they were assessed with the solid media, whereas only 6 of these isolates were resistant to 0.1 μg/ml of INH when they were tested by the broth method.

Two-temperature PCR. We optimized a two-temperature PCR strategy to amplify regions of eight drug resistance-related genes in *M. tuberculosis*. The target regions varied in length from 315 to 2,748 bp (Table 2). Genomic DNA (approximately 100 ng) from *M. tuberculosis* strain H37Rv was amplified with eight primer pairs simultaneously. The entire procedure, including PCR, took less than 60 min. PCR products were separated by electrophoresis on 1% agarose gels and stained with ethidium bromide (Fig. 1A). Genomic DNAs from strain H37Ra and 138 clinical isolates of *M. tuberculosis*

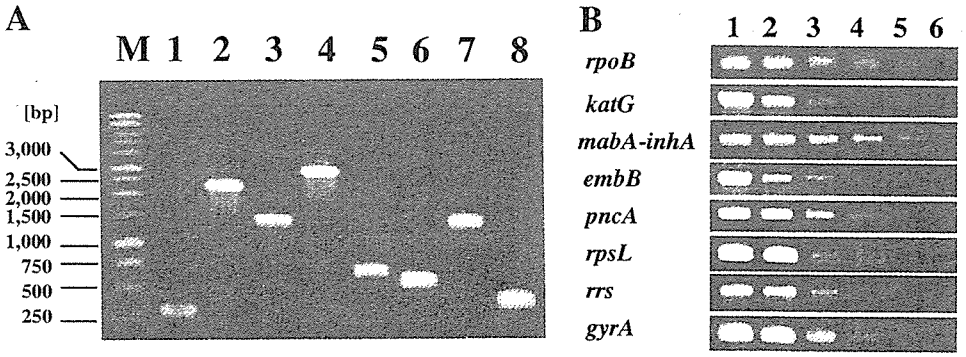

FIG. 1. (A) Amplification products from two-temperature PCR of *M. tuberculosis* H37Rv. PCR products were separated by electrophoresis on 1% agarose gels and stained with ethidium bromide. Lane M, 1-kbp ladder as a molecular size marker; lane 1, *rpoB*; lane 2, *katG*; lane 3, *mabA-inhA* locus; lane 4, *embB*; lane 5, *pncA*; lane 6, *rpsL*; lane 7, *rrs*; and lane 8, *gyrA*. (B) Determination of the sensitivity of two-temperature PCR with serially diluted *M. tuberculosis* H37Rv DNA as a template. Experiments were repeated twice with similar results. Lane 1, 100 ng of template DNA; lane 2, 10 ng; lane 3, 1 ng; lane 4, 100 pg; lane 5, 10 pg; lane 6, 1 pg.

were then amplified by PCR. Each PCR yielded a single band of the expected length (data not shown). These results indicate that the PCR is reliable for use in clinical isolates of *M. tuberculosis*.

Sensitivity and specificity of two-temperature PCR. To determine the sensitivity of the two-temperature PCR for the target DNA, 100, 10, and 1 ng and 100, 10, and 1 pg of genomic DNA from *M. tuberculosis* H37Rv were amplified with the PCR assay. As shown in Fig. 1B, the limits of detection for *mabA-inhA* and *rpoB*, for *gyrA*, *pncA*, and *rpsL*, and for *embB*, *katG*, and *rrs* were 10 pg, 100 pg, and 1 ng of DNA, respectively.

To determine the species specificity of the PCR, genomic DNA (100 ng) was isolated from various species of bacteria, including *Mycobacterium* spp. and additional pathogenic bacterial species listed in Table 1. DNA was amplified with the PCR primer pairs shown in Table 2. The PCR patterns for *M. bovis* BCG were identical to those of *M. tuberculosis* (Table 3). Some mycobacterial species were positive for the PCR with primer pairs for *rpsL*, *rrs*, and *gyrA*; however, all mycobacterial species except *M. tuberculosis* and *M. bovis* were negative for *rpoB*-, *katG*-, *mabA*-, *embB*-, and *pncA*-specific PCR products (Table 3). Nonmycobacterial strains tested were negative for all eight gene targets.

Sequencing of *rpoB*, *katG*, *mabA-inhA*, *embB*, *pncA*, *rpsL*, *rrs*, and *gyrA* of *M. tuberculosis*. PCR products were purified and then sequenced with the 16 sequencing primers listed in Table 2. Sequencing yielded 8.8 kb of sequence for each *M. tuberculosis* strain. Sequences were obtained for regions of the *rpoB*, *katG*, *mabA*, *embB*, *pncA*, *rpsL*, *rrs*, and *gyrA* genes and the promoters of *mabA-inhA* and *pncA*. The mutations identified in the 138 clinical isolates of *M. tuberculosis* are shown in Table 4.

(i) *rpoB*. We sequenced a 240-bp fragment containing the "81-bp core region" of *rpoB*. One hundred nine isolates had no mutations in *rpoB*. The remaining 25 each had a single point mutation, and 4 isolates each had two point mutations. All of the detected mutations resulted in amino acid substitutions. Of these mutations, two, S450L (TCG→TTG at nucleotide [nt] positions 1348 to 1350) and S509R (AGC→AGG at nt positions 1525 to 1527) were novel (Table 4).

(ii) *katG*. Thirty-seven isolates had no mutations in *katG*, whereas 81 isolates each had a single point mutation, 11 isolates had two point mutations each, 1 isolate had three point mutations, and 2 isolates had a 3-bp insertion each. One mutation was a silent mutation (CTG→TTG at nt positions 1957 to 1959 [L653L]), and all others caused amino acid substitutions. We identified 10 novel point mutations and the novel L390 insertion.

(iii) *mabA-inhA* locus. We found no mutations in the *mabA* gene and the regulatory region of *mabA-inhA* in 126 isolates. Ten isolates had a C-to-T transition −15 bp upstream of the *mabA* initiation codon, 1 isolate had a T-to-A transition 8 bp upstream of the initiation codon, and 1 isolate had a T-to-A transition 5 bp upstream of the initiation codon. The T-to-A transition −5 bp upstream of the initiation codon was novel.

(iv) *embB*. We found no mutations in *embB* in 107 isolates. Twenty-six isolates each had a single point mutation, 3 each had two point mutations, and 2 each had three point mutations. Several isolates had silent mutations (D345D, D534D, L355L, and P1075P). Five of these point mutations were novel.

(v) *pncA*. One hundred nineteen isolates had no mutations in *pncA* or the *pncA* regulatory region. Nineteen isolates each had a single point mutation. Five of these mutations were novel.

(vi) *gyrA*. All isolates tested contained the E21Q mutation of *gyrA*. Eighteen isolates each had one point mutation, 117 isolates each had two point mutations, 2 isolates each had three point mutations, and 1 isolate carried four mutations.

(vii) *rpsL*. All isolates carried the K121K mutation of *rpsL*. One hundred twenty-five isolates each had a single point mutation, and the remaining 13 isolates each had two point mutations.

(viii) *rrs*. One hundred thirty-three isolates had no mutations in *rrs*. Two isolates had a C-to-T transition at nt position 516. One isolate had an A-to-G transition at nt position 1400. One isolate had two point mutations, an A-to-G transition at nt position 1400 and an A-to-G transition at nt position 1539. One isolate had an insertion of a cytosine at position 1061 of *rrs*.

TABLE 3. Species specificity of two-temperature PCR

Bacterium	Origin	Results of PCR with various primer pairs[g]							
		rpoB	*katG*	*mabA-inhA*	*embB*	*pncA*	*rpsL*	*rrs*	*gyrA*
M. tuberculosis IMCJ	105 clinical isolates from Japan	+	+	+	+	+	+	+	+
M. tuberculosis P	33 clinical isolates from Poland	+	+	+	+	+	+	+	+
M. tuberculosis H37Rv	ATCC[a] 27294	+	+	+	+	+	+	+	+
M. tuberculosis H37Ra	ATCC 25177	+	+	+	+	+	+	+	+
M. bovis BCG Japanese strain 172	Japan BCG Laboratory[b]	+	+	+	+	+	+	+	+
M. avium	ATCC 25291	−	−	−	−	−	+	+	−
M. gastri	GTC[c] 610 (ATCC 15754)	−	−	−	−	−	+	+	+
M. intracellulare	JCM[d] 6384 (ATCC 13950)	−	−	−	−	−	+	+	−
M. kansassii	JCM 6379 (ATCC 124878)	−	−	−	−	−	+	+	−
M. marinum	GTC 616 (ATCC 927)	−	−	−	−	−	+	+	+
M. simiae	GTC 620 (ATCC 25275)	−	−	−	−	−	−	−	+
M. scrofulaceum	JCM 6381 (ATCC 19981)	−	−	−	−	−	−	+	−
M. szulgai	JCM 6383 (ATCC 35799)	−	−	−	−	−	+	+	+
M. nonchromogenicum	JCM 6364 (ATCC 19530)	−	−	−	−	−	+	−	−
M. terrae	GTC 623 (ATCC 15755)	−	−	−	−	−	−	−	−
M. chelonae	JCM 6390 (ATCC 14472)	−	−	−	−	−	+	−	−
M. fortuitum	RIMD[e] 1317004 (ATCC 6841)	−	−	−	−	−	+	−	−
M. phlei	RIMD 1326001 (ATCC 19249)	−	−	−	−	−	−	−	−
M. smegmatis	ATCC 19420	−	−	−	−	−	+	−	−
Escherichia coli	ATCC 8739	−	−	−	−	−	−	−	−
Haemophilus influenzae	IID[f] 984 (ATCC 9334)	−	−	−	−	−	−	−	−
Klebsiella pneumoniae	IID5209 (ATCC 15380)	−	−	−	−	−	−	−	−
Legionella pneumophila	GTC 745	−	−	−	−	−	−	−	−
Mycoplasma pneumoniae	IID 817	−	−	−	−	−	−	−	−
Pseudomonas aeruginosa	ATCC 27853	−	−	−	−	−	−	−	−
Rhodococcus equi	ATCC 33710	−	−	−	−	−	−	−	−
Staphylococcus aureus	N315	−	−	−	−	−	−	−	−
Streptococcus pneumoniae	GTC 261	−	−	−	−	−	−	−	−

[a] American Type Culture Collection, Rockville, MD.
[b] Japan BCG Laboratory, Tokyo, Japan.
[c] Gifu Type Culture Collection, Department of Microbiology-Bioinformatics, Regeneration and Advanced Medical Science, Gifu University, Graduate School of Medicine, Bacterial Genetic Resources, Gifu, Japan.
[d] Japan Collection of Microorganisms, Institute of Physical and Chemical Research (RIKEN), Saitama, Japan.
[e] Research Institute for Microbial Diseases, Osaka University, Osaka, Japan.
[f] Institute of Medical Science, University of Tokyo, Tokyo, Japan.
[g] Amplification results were determined by agarose gel electrophoresis. Symbols: +, presence of amplification products; −, absence of amplification products.

Correlation between drug susceptibility and mutation(s) in *M. tuberculosis*. (i) RIF resistance and *rpoB*. Mutations in the 81-bp core region of *rpoB* are responsible for resistance in at least 96% of RIF-resistant *M. tuberculosis* isolates (17, 31, 39). In the present study, we identified two novel mutations, S450L (TCG→TTG at nt positions 1348 to 1350) and S509R (AGC→AGG at nt positions 1525 to 1527). S450L was located upstream of the 81-bp core region, and the isolate with S450L was susceptible to RIF, indicating this mutation is not associated with RIF resistance. Isolates with both S509R and H526R (CAC→CGC at nt positions 1576 to 1578) mutations were RIF resistant. However, it is unclear whether S509R is associated with RIF resistance because H526R is known to be associated with RIF resistance (39).

(ii) INH resistance and *katG* and *mabA-inhA*. INH resistance is related to mutation(s) in *katG*, *inhA*, and/or the promoter region of *mabA-inhA* (17, 22, 38, 39). In the present study, we found 11 novel mutations and a CTA insertion at nt position 1170 in *katG*. Among these mutations, Q295P and G297V conferred INH resistance. Two INH-resistant isolates carried the L141F and R463L mutations. R463L is known not to be associated with INH resistance (33, 39), and L141F may confer INH resistance. The A65T, A245V, and V725A mutations did not influence INH susceptibility. Isolates carrying the T324P, L48Q, or M257T mutation and −15C→T upstream of *mabA* were resistant to INH. However, it is unclear whether T324P, L48Q, or M257T is related to INH resistance because the −15C→T upstream of *mabA* is known to confer INH resistance (10, 22, 39).

(iii) EMB resistance and *embB*. EMB resistance is related to mutations in *embB* (17, 32, 39). In the present study, we found five novel mutations in *embB*. Among these, D354A conferred EMB resistance. V492L, A680T, and A1007V were not associated with EMB resistance. An isolate with both N296Y and M306I was resistant to EMB. However, it is unclear whether N296Y is related to EMB resistance because the M306I mutation is known to confer EMB resistance (39).

(iv) PZA resistance and *pncA*. It is known that PZA resistance is related to mutations in *pncA* (17, 26, 39). In the present study, we identified five novel mutations in *pncA*. Among these, A3E, D53N, P54L, C72W, and M175V conferred PZA resistance. It will be necessary to determine whether the PZA activities of various mutants are correlated with PZA susceptibility. We then evaluated the PZase activities of *M. tuberculosis* clinical isolates, strains H37Rv and H37Ra, and *M. bovis* strain BCG. The BCG strain was included as a negative control as described in Materials and Methods. One hundred twenty-one clinical isolates and H37Rv

TABLE 4. Nucleotide and amino acid changes found in 138 clinical isolates of *M. tuberculosis*[a]

Gene	No. of isolates (n = 138)	Isolate origin	Changes		% Resistant (no. of isolates displaying resistance)	Other mutations
			Nucleotide	Amino acid (silent mutation)		
rpoB[b]	83	Japan	None	None	0	
	26	Poland	None	None	0	
	1	Japan	TCG→TTG	S450L*	0	
	1	Poland	CAA→CTA	Q513L	100	
	1	Japan	GAC→GTC	D516V	100	
	1	Japan	TCG→TTG	S522L	100	
	1	Japan	CAC→TAC	H526Y	100	
	2	Japan	CAC→CGC	H526R	100	
	1	Poland	CAC→ACC	H526T	100	
	7	Japan	TCG→TTG	S531L	100	
	5	Japan	TCG→TGG	S531W	100	
	5	Poland	TCG→TTG	S531L	100	
	2	Japan	AGC→AGG and CAC→CGC	S509R* and H526R	100	
	2	Japan	ATG→ATT and GAC→TAC	M515I and D516Y	100	
katG	14	Japan	None	None	0	
	23	Poland	None	None	4.4 (1)	
	1	Japan	CTG→TTG	(L653L)	0	
	1	Japan	GCC→ACC	A65T*	0	
	1	Japan	GCG→CTG	A245V*	0	
	1	Poland	CAG→CCG	Q295P*	100	
	1	Poland	GGC→GTC	G297V*	100	
	4	Japan	AGC→ACC	S315T	100	
	2	Japan	AGC→AAC	S315N	100	
	3	Poland	AGC→ACC	S315T	100	
	1	Japan	GTC→GCC	V725A*	0	
	63	Japan	CGG→CTG	R463L	3.2 (2)	
	2	Japan	CGG→CTG	R463L	100	−15C→T upstream of *mabA*
	1	Poland	ACC→CCC	T324P*	100	−15C→T upstream of *mabA*
	7	Japan	AGC→ACC and CGG→CTG	S315T and R463L	100	
	2	Japan	TTG→TTC and CGG→CTG	L141F* and R463L	100	
	1	Japan	ATG→ACG and CGG→CTG	M257T* and R463L	100	−5T→A* upstream of *mabA*
	1	Japan	CTG→CAG and CGG→CTG	L48Q* and R463L	100	−15C→T upstream of *mabA*
	1	Japan	ATG→ACG, CGG→CTG, and GTC→GCC	M257T*, R463L and V708P*	100	−15C→T upstream of *mabA*
	2	Japan	CTA insertion at position 1170	L390 insertion*	100	
mabA-inhA operon[c]	97	Japan	None	None	0	
	29	Poland	None	None	3.4 (1)	
	2	Japan	−15C→T upstream of *mabA*	None	100	R463L in *katG*
	1	Poland	−15C→T upstream of *mabA*	None	100	T324P* in *katG*
	1	Japan	−15C→T upstream of *mabA*	None	100	L48Q* and R463L in *katG*
	1	Japan	−15C→T upstream of *mabA*	None	100	M257T*, R463L and V708P* in *katG*
	1	Japan	−15C→T upstream of *mabA*	None	100	
	4	Poland	−15C→T upstream of *mabA*	None	100	
	1	Japan	−8T→A upstream of *mabA*	None	100	
	1	Japan	−5T→A* upstream of *mabA*	None	100	M257T* and R463L in *katG*
embB	77	Japan	None	None	0	
	30	Poland	None	None	3.3 (1)	
	2	Japan	GAC→GAT	(D345D)	100 (2)	
	1	Japan	GAC→GAT	(D534D)	0	
	5	Japan	ATG→GTG	M306V	100	
	1	Japan	ATG→ATT	M306I	100	
	1	Japan	ATG→ATC	M306I	100	
	2	Poland	ATG→ATA	M306I	100	
	2	Japan	GAC→GCC	D354A*	100	

Continued on following page

TABLE 4—*Continued*

Gene	No. of isolates (n = 138)	Isolate origin	Changes		% Resistant (no. of isolates displaying resistance)	Other mutations
			Nucleotide	Amino acid (silent mutation)		
	4	Japan	GAG→GCG	E378A	0	
	1	Japan	GTG→TTG	V492L*	0	
	1	Poland	CAG→CGG	Q497R	100	
	2	Japan	GCC→ACC	A680T*	0	
	3	Japan	GCC→GTC	A1007V*	0	
	1	Japan	GAC→AAC	D1024N	0	
	2	Japan	CTG→CTA and GAG→GCG	(L355L) and E378A	0	
	1	Japan	AAT→TAT and ATG→ATA	N296Y* and M306I	100	
	2	Japan	ATG→CTG, GAG→GCG, and CCC→CCA	M306L, E378A, and (P1075P)	100	
pncA	89	Japan	None	None	0	
	30	Poland	None	None	0	
	2	Japan	TCC→TCT	(S65S)	0	
	1	Japan	GCG→GAG	A3E*	100	
	1	Poland	CAG→CCG	Q10P	100	
	1	Japan	GAC→GCC	D12A	100	
	2	Japan	CAC→CAA	H51Q	100	
	1	Poland	CAC→CAG	H51Q	100	
	3	Japan	CCG→CTG	P54L*	100	
	1	Japan	TGC→TGG	C72W*	100	
	2	Japan	GGT→AGT	G132S	100	
	2	Japan	ATT→ACT	I133T	100	
	1	Poland	CGC→AGC	R148S	100	
	1	Japan	ATG→GTG	M175V*	100	
	1	Japan	GAC→AAC	D53N*	100	
gyrA	7	Japan	GAG→CAG	E21Q*	0	
	11	Poland	GAG→CAG	E21Q*	0	
	95	Japan	GAG→CAG and AGC→ACC	E21Q* and S95T	0	
	22	Poland	GAG→CAG and AGC→ACC	E21Q* and S95T	0	
	1	Japan	GAG→CAG, GAC→GGC, and AGC→ACC	E21Q*, D94G, and S95T	100	
	1	Japan	GAG→CAG, GCG→GTG, and AGC→ACC	E21Q*, A90V, and S95T	100	
	1	Japan	GAG→CAG, GCG→GTG, GAC→GCC, and AGC→ACC	E21Q*, A90V, D94A, and S95T	100	
rpsL	87	Japan	AAA→AAG	(K121K)	11.5 (10)	
	33	Poland	AAA→AAG	(K121K)	6.1 (2)	
	2	Japan	AAA→AAG	(K121K)	100	516C→T in *rrs*
	1	Japan	AAA→AAG	(K121K)	100	1,061C insertion* in *rrs*
	1	Japan	AAA→AAG	(K121K)	100	1,400A→G in *rrs*
	1	Japan	AAA→AAG	(K121K)	100	1,400A→G and 1539A→G in *rrs*
	13	Japan	AAG→AGG and AAA→AAG	K43R and (K121K)	100	
rrs	33	Poland	None		6.1 (2)	(K121K) in *rpsL*
	87	Japan	None		11.5 (10)	(K121K) in *rpsL*
	13	Japan	None		100	K43R and (K121K) in *rpsL*
	2	Japan	516C→T		100	(K121K) in *rpsL*
	1	Japan	1,061C insertion*		100	(K121K) in *rpsL*
	1	Japan	1,400A→G		100	(K121K) in *rpsL*
	1	Japan	1,400A→G and 1539A→G		100	(K121K) in *rpsL*

[a] *, mutation not previously reported.
[b] The codon numbering system of RpoB initially described by Telenti et al. (31) was used. The codon numbers of RpoB are designated on the basis of alignment of translated *E. coli rpoB* sequence with a portion of translated *M. tuberculosis* sequence and are not the positions of the actual *M. tuberculosis rpoB* codons.
[c] Nucleotide numbering based on nucleotide position relative to *mabA* start codon.

and H37Ra were positive for PZase activity (data not shown). The remaining 17 *M. tuberculosis* clinical isolates and *M. bovis* BCG were negative for PZase activity. All PZase-positive bacilli were sensitive to PZA, and all PZase-negative bacilli were resistant to PZA. These data were consistent with previously published results (15, 39).

(v) **STR resistance and *rpsL* and *rrs*.** STR resistance is related to mutations in *rpsL* and *rrs* (17, 19, 39). In the present

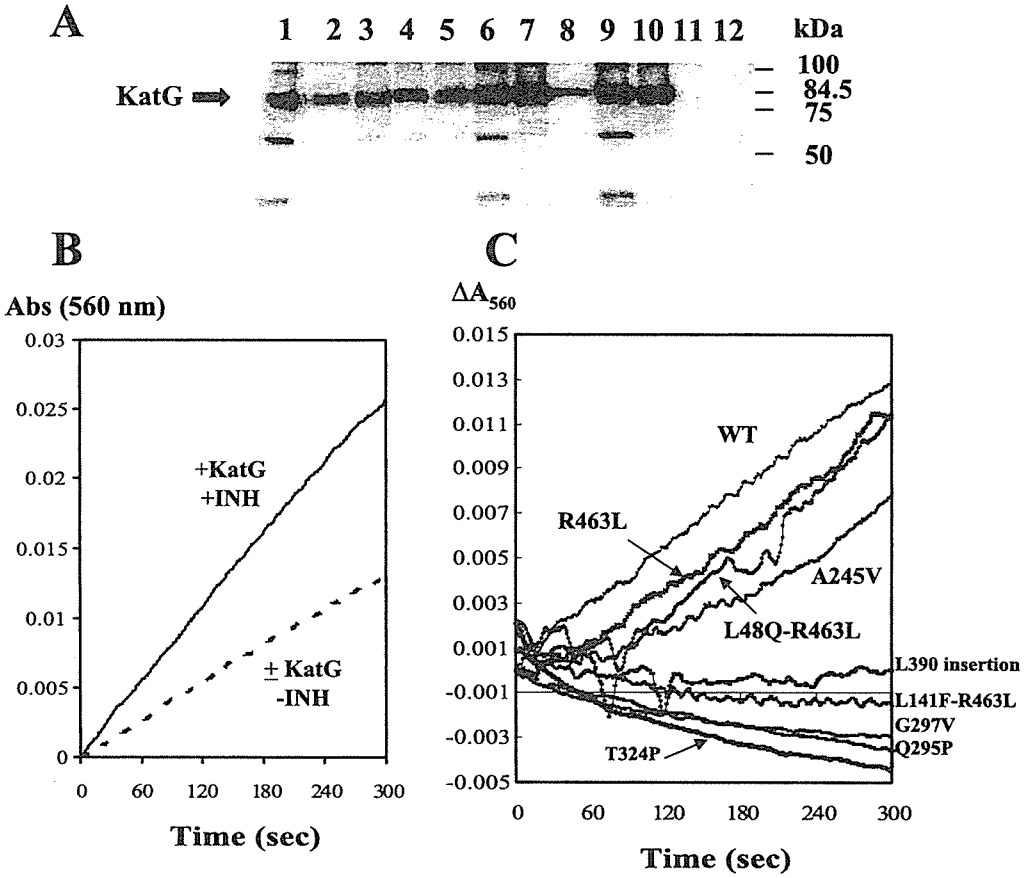

FIG. 2. (A) Western blot analysis of whole-cell protein extracts from KatG-deficient *E. coli* strain UM262 complemented with a control plasmid, pCRT7/NT, or recombinant plasmids expressing various KatG mutants. Lane 1, wild-type KatG; lane 2, KatG^{Q295P}; lane 3, KatG^{T324P}; lane 4, KatG$^{L48Q\text{-}R463L}$; lane 5, KatG^{R463L}; lane 6, KatG^{G297V}; lane 7, KatG^{A245V}; lane 8, KatG$^{L390\ insertion}$; lane 9, KatG$^{L141F\text{-}R463L}$; lane 10, purified KatG protein; lane 11, control plasmid pCRT7/NT; and lane 12, *E. coli* strain UM262. The positions of molecular mass markers are shown. (B) Time course of NBT reduction with and without the addition of 2.4 mM INH with wild-type KatG. Abs, absorbance. (C) Time course of net INH-dependent NBT reduction by wild-type KatG (WT) and eight KatG mutants. For each KatG sample tested, NBT reduction in the absence of INH was subtracted from that in the presence of INH to obtain the net INH-dependent NBT reduction over time. The concentration of KatG was determined by enzyme-linked immunosorbent assay.

study, all isolates, regardless of STR resistance status, had a silent mutation (K121K) in *rpsL*, and, therefore, the K121K mutation is not associated with STR resistance.

We found a novel insertional mutation in *rrs*. The insertion is the likely cause of STR resistance, because the isolate with the mutation was resistant to STR.

(vi) FQ resistance and *gyrA*. Mutations in the FQ resistance-determining region (QRDR) in *gyrA* are responsible for resistance in at least 96% of FQ-resistant *M. tuberculosis* isolates (17, 30, 39). In the present study, we found one novel mutation, E21Q, in *gyrA*, and all isolates tested, except the H37Rv strain, contained this mutation. However, some isolates were susceptible to FQs and others were resistant. Therefore, it is not clear that this mutation is associated with resistance to FQs. E21Q is located upstream of the QRDR.

Catalase and INH oxidation activities of recombinant KatG mutants. KatG, catalase-peroxidase, converts INH to its biologically active form (38). Some mutations in *katG* reduce or eliminate the enzymatic activity that is associated with INH resistance (9, 39). To measure catalase and INH oxidation activities, we expressed wild-type KatG and the A245V, Q295P, G297V, T324P, L48Q-R463L, L141F-R463L, R463L, and L390 insertion mutants of KatG in *katG*-deficient *E. coli* (Fig. 2A and Table 5). The catalase activities of these mutants were determined at various H_2O_2 concentrations. The k_{cat}, K_m, and k_{cat}/K_m ratio values are shown in Table 5. Catalase activity was not detected for the KatG^{Q295P}, KatG^{G297V}, KatG^{T324P}, KatG$^{L141F\text{-}R463L}$, or KatG$^{L390\ insertion}$ mutants. The k_{cat} of the KatG$^{L48Q\text{-}R463L}$ mutant was 26% lower than that of wild-type KatG. In contrast, the KatG^{A245V} and KatG^{R463L} mutants showed activities similar to that of wild-type KatG.

The INH oxidation activities of the mutants were determined in the presence of H_2O_2 by monitoring the free radical generation in the NBT reduction reaction. When wild-type KatG was tested in this assay, there was a significant background activity of NBT reduction in the absence of INH, whereas the NBT reduction was increased significantly in the presence of INH (Fig. 2B). We subtracted the background activity to obtain the net INH oxidation/NBT reduction. The net values are shown in Fig. 2C. The KatG^{Q295P}, KatG^{G297V}, KatG^{T324P}, KatG$^{L141F\text{-}R463L}$, and KatG$^{L390\ insertion}$ mutants did not show enhanced activity, whereas wild-type KatG and

TABLE 5. Catalase activity of wild-type and mutant KatG, KatG-mediated INH-converting activity, and INH susceptibility

Recombinant KatG[a]	Catalase activity			KatG-mediated INH-converting activity[b]	INH susceptibility[c]
	k_{cat} (S^{-1})	K_m (mM)	k_{cat}/K_m ratio (mutant/wild type)		
Wild type	2,403 ± 440	60.1 ± 9.5	1.00	+	S
A245V*	2,666 ± 530	62.8 ± 10.8	1.06	+	S
Q295P*	ND[d]	ND	NA[e]	−	R
G297V*	188 ± 36	68.7 ± 7.0	0.07	−	R
T324P*	ND	ND	NA	−	R
L48Q*-R463L	1,776 ± 310	64.8 ± 12.5	0.69	+	R
L141F*-R463L	ND	ND	NA	−	R
R463L	2543 ± 450	64.0 ± 11.0	1.01	+	S
L390 (CTA) insertion*	ND	ND	NA	−	R

[a] *, novel mutation.
[b] Time courses of net KatG-mediated INH conversion are shown in Fig. 2C.
[c] INH susceptibilities shown are those of *M. tuberculosis* H37Rv strains having the *katG* gene of the wild type and those of clinical strains having the *katG* gene with the respective mutation(s). S, susceptible; R, resistant.
[d] ND, not detected.
[e] NA, not applicable.

the $KatG^{L48Q\text{-}R463L}$, $KatG^{A245V}$, and $KatG^{R463L}$ mutants of KatG showed significant enhancement of activity in the presence of INH.

Collectively, these results for the enzymatic activities of KatG mutants indicate that the Q295P, G297V, T324P, L141F, and L390 insertion mutants cause loss of enzymatic activity, whereas the A245V and R463L mutants have no effect on the enzymatic activity. The L48Q mutation has little effect on enzymatic activity; however, there was no isolate that carried only the L48Q mutation in KatG in the present study. These mutations and enzymatic activities, except for those of the L48Q-R463L mutant, correlated well with INH susceptibility (Table 5). The L48Q-R463L mutant also carried the −15C→T transition upstream of *mabA* (Table 4). Therefore, the INH resistance of this mutant is likely due to the −15C→T mutation, which is known to be related to INH resistance (10, 22, 39).

Sequencing of *rpoB*, *katG*, *mabA-inhA*, *embB*, *pncA*, *rpsL*, *rrs*, and *gyrA* of *M. bovis* BCG. PCR products amplified from *rpoB*, *katG*, *mabA-inhA*, *embB*, *pncA*, *rpsL*, *rrs*, and *gyrA* of *M. bovis* BCG were sequenced with the same sequencing primers as those for *M. tuberculosis* (Table 2). When the nucleotide sequences of BCG were compared with those of *M. bovis* AF2122/97 (GenBank accession no. NC_002945) (8), the sequences were identical. When the sequences of *M. bovis* BCG were compared with those of *M. tuberculosis* H37Rv, the sequences of *rpoB*, the promoter region of the *mabA-inhA* operon, and *rrs* were identical. The R463L (CGG→CTG at nt positions 1387 to 1389) and silent P29P (CCC→CCA at nt positions 85 to 87) mutations were found in *katG* of BCG. E378A (GAG→GCG at nt positions 1159 to 1161) in *embB*, H57D (CAC→GAC at nt positions 169 to 171) in *pncA*, K121K (AAA→AAG at nt positions 361 to 363 [silent]) in *rpsL*, and S95T (AGC→ACC at nt positions 283 to 285) in *gyrA* were identified in *M. bovis* BCG.

Correlation between drug susceptibility and mutations in BCG. We next compared the sequences of BCG and *M. tuberculosis* H37Rv and found four mutations, R463L in *katG*, E378A in *embB*, H57D in *pncA*, and S95T in *gyrA*, that caused amino acid substitutions in *M. bovis* BCG. R463L in *katG* is known not to be associated with INH resistance in *M. tuberculosis* (33) and may not be associated with INH resistance in *M. bovis*. E378A in *embB* is not associated with EMB resistance in *M. tuberculosis* (32, 39). H57D in *pncA* was reported previously and is characteristic of PZA resistance in *M. bovis* (39). S95T in *gyrA* is not associated with FQ resistance in *M. tuberculosis* (39). Therefore, in *M. bovis*, mutations except H57D in *pncA* may be polymorphisms not associated with drug resistance.

Detection and sequencing of drug resistance-related genes of *M. tuberculosis* in sputa from tubercular patients. We tested a total of 10 sputa from 10 tuberculosis-diagnosed patients. These patients had been received treatment with antitubercular drugs. Of these samples, six were positive for acid-fast bacilli (AFB; >101/field in two samples, 26 to 50/field in two samples, 1/field in one sample, and 1/several fields in one sample) under microscopic observation, and four were negative. Five of the six samples that were positive for AFB were positive for all eight genes tested by PCR. One sample which was positive for AFB (one/several fields) was positive for five genes (*rpoB*, *pncA*, *rpsL*, *rrs*, and *gyrA*) by PCR. The four AFB-negative samples yielded no PCR products and were negative by culture, suggesting that tuberculosis was not active in these patients who had received treatment.

PCR products (a total of 45) were subjected to DNA sequencing. No mutations were identified in 38 of the PCR products. The remaining seven PCR products contained nine mutations. The seven PCR products were obtained from one sputum sample. The sputum sample was cultured, and after several weeks, an isolate of *M. tuberculosis* was obtained and analyzed. We conducted PCR analysis of this isolate and detected the same nine mutations. This isolate was resistant to RIF, INH, EMB, STR, FQs, and PZA. These results indicate that our DNA sequencing-based method can be used to detect MDR strains of *M. tuberculosis* in sputa obtained from clinical tuberculosis patients.

DISCUSSION

Our novel DNA sequencing-based method described here is useful for detection and diagnosis of drug-resistant strains of *M. tuberculosis*, especially MDR strains. Our method has

several advantages. First, it allows simultaneous detection of mutations in eight genes associated with resistance to six antituberculosis drugs. Second, the entire assay from DNA extraction to the DNA sequencing can be completed within 1 working day. Third, this method is sensitive enough to detect 1 ng of genomic DNA (i.e., 3×10^5 *M. tuberculosis* cells). We found that this method worked well even in positive sputum containing few bacilli, as determined by acid-fast staining. Fourth, our DNA sequencing-based method allows detection of both novel and known mutations. In the present study, we identified 25 novel mutations by PCR-based analysis.

This strategy does have a few disadvantages. The DNA sequencer and sequencing are costly, and the procedure is somewhat complicated. However, this issue may be addressed if DNA sequencing costs are reduced by new sequencing methods and equipment. Also, this strategy may not be able to detect very low numbers of bacilli in sputa. We did not have the opportunity to test AFB smear-negative but culture-positive samples. Among the smear- and culture-positive samples we tested, one sample with small numbers of bacilli (one/several fields) was negative for three of the eight genes tested, indicating that the sensitivity of this method is limited. However, the sensitivity and accuracy of our method are comparable to those of traditional drug susceptibility tests, and this is sufficient for use in the clinical setting.

The method described here was excellent for diagnosis of RIF-resistant *M. tuberculosis* isolates with 100% specificity, sensitivity, and test efficiency. RIF interferes with the synthesis of mRNA by binding to the β-subunit of RNA polymerase (RpoB) in bacterial cells (39). The RIF-binding site is a pocket in the upper wall of the main channel for double-stranded DNA entry just upstream of the polymerase catalytic center. The various RIF-resistant mutations are clustered around this pocket (39). Mutations in *rpoB* have been found in 95% to 100% of clinical RIF-resistant isolates of *M. tuberculosis* (39). Most of the mutations found in the 28 RIF-resistant isolates tested here were located between nucleotides 1276 and 1356 (codons 507 to 533) of *rpoB*, which is the 81-bp core region of this gene (Table 4) (31, 39). Two other mutations, V146F and E562A, were located outside of the 81-bp core region. Isolates with V146F were reported to show low-level resistance to RIF (MIC, ≤4 μg/ml) (39). It is not known whether the E562A mutation is involved in resistance because the isolate with this mutation also had another mutation in the 81-bp core region (39). The V146F mutation could not be detected by the DNA sequencing method described here. Although we were able to detect the E562A mutation by our sequencing method, we did not find this mutation in any of 138 isolates tested in the present study.

Our sequencing method is applicable for diagnosis of INH-resistant isolates with 89.5% sensitivity, 100% specificity, and 97.1% test efficiency (Table 6). The sensitivity of the two-temperature PCR for *katG* was lower than that of the PCR for *rpoB* or *mabA-inhA* (Fig. 1B), and, therefore, we will need to increase the sensitivity to detect *katG* mutations to assess INH resistance. The mode of INH action is one of the most complicated among all antibiotics. INH is a prodrug that requires activation of the bacterial catalase-peroxidase enzyme (KatG) (38) to generate a range of reactive radicals, which then affect multiple systems, including cell wall mycolic acid synthesis and lipid peroxidation and NAD metabolism, and cause DNA damage (39). Deficient efflux of INH radicals and defective antioxidative defenses may underlie the susceptibility of *M. tuberculosis* to INH (39). Mutations in *katG* are among the most frequently detected mutations in INH-resistant clinical isolates. Mutations in *inhA* and its promoter region, which is located upstream of the *mabA-inhA* operon, are also common (16, 17, 39). Our sequencing method should identify a majority of INH-resistant isolates. We are able to detect mutations in *katG* and the region upstream of *mabA* in 90% (34/38) of INH-resistant isolates. Ten different mutations (L48Q, L141F, M257T, Q295P, G297V, S315T, S315N, T324P, R463L, and V708P) were detected in *katG* of INH-resistant isolates, and 3 mutations (A65T, A245V, and V725A) were identified in INH-susceptible isolates. The L48Q, A65T, L141F, A245V, M257T, Q295P, G297V, T324P, V708P, V725A, and L390 insertion mutations are novel (Table 4).

To date, several mutations in *katG* in MDR isolates have been reported (9, 16, 17, 38, 39). Rouse et al. (24) reported previously that codons 104 and 108 encode amino acids located near the catalytic site of KatG and that the residues encoded by codons 270, 275, and 315 participate in binding the heme group

TABLE 6. The diagnostic performance of the DNA sequencing-based method in comparison with drug susceptibility testing[a]

Drug susceptibility test result[b]	No. of isolates (n = 138)		% Sensitivity[c]	% Specificity[d]	% Test efficiency[e]
	Mutation positive	Mutation negative			
RIF					
Resistant	28	0	100	100	100
Susceptible	0	110			
INH					
Resistant	34	4	89.5	100	97.1
Susceptible	0	100			
EMB					
Resistant	15	3	83.3	100	97.8
Susceptible	0	120			
PZA					
Resistant	17	0	100	100	100
Susceptible	0	121			
STR					
Resistant	18	12	60.0	100	91.3
Susceptible	0	108			
OFX					
Resistant	3	0	100	100	100
Susceptible	0	135			

[a] The diagnostic performance of the DNA sequencing-based method in comparison with drug susceptibility testing was determined after resolution of polymorphisms.

[b] Drug susceptibility for antituberculosis agents except for PZA was determined by the agar proportion method according to NCCLS (now CLSI) guidelines, and that for PZA was determined by PZase activity.

[c] Sensitivity: no. of drug-resistant isolates with mutations/(no. of drug-resistant isolates with mutations + no. of drug-resistant isolates without mutations).

[d] Specificity: no. of drug-susceptible isolates without mutations/(no. of drug-susceptible isolates with mutations + no. of drug-susceptible isolates without mutations).

[e] Test efficiency: (no. of drug-resistant isolates with mutations + no. of drug-susceptible isolates without mutations)/no. of all isolates tested.

of KatG (24). Mutations in these regions, therefore, are thought to cause loss of KatG enzymatic function (24). Yu et al. (36) reported that residue W321 of KatG was important for substrate binding and that residue Y229 was critical to protect the catalase activity of KatG (37). We compared the catalase and INH oxidation activities of eight KatG mutants identified in this study with those of the wild type. Although we were able to express all of the KatG mutants (Fig. 2A), we were unable to detect the catalase and INH oxidation activities of four KatG mutants, $KatG^{Q295P}$, $KatG^{T324P}$, $KatG^{L141F\text{-}R463L}$, and $KatG^{L390\ insertion}$ (Table 5 and Fig. 2C). The specific effects of these mutations on KatG function need to be analyzed further. The lack of activity or lower activity of these mutants, however, correlated quite well with the INH-resistant phenotype of their respective *M. tuberculosis* isolates. The enzymatic activity of $KatG^{L48Q\text{-}R463L}$ was not correlated with INH susceptibility (Table 5), and this mutation had little effect on the measured activities (Table 5 and Fig. 2C). The isolate carrying the L48Q-R463L mutations also had the −15C→T transition upstream of *mabA* (Table 4), which is known to be associated with INH resistance (10, 22, 39). The $KatG^{A245V}$ and $KatG^{R463L}$ mutants showed activities similar to those of wild-type KatG, and these results are consistent with the INH-susceptibility phenotypes of their respective isolates. Therefore, we concluded that the L48Q, A245V, and R463L mutations are merely polymorphisms that do not influence INH resistance.

We found mutations in the region upstream of *mabA* or in the regulatory region of the *mabA-inhA* operon in 12 of 38 INH-resistant isolates. Five of these isolates had no other mutations within *katG* (Table 4). Our present results support those of Morris et al. (16), who examined the *inhA* locus for sequence polymorphisms by single-strand conformation polymorphism analysis and DNA sequencing of 42 INH-resistant isolates. They found no alterations in the coding portion of *inhA*, but five isolates had mutations in the regulatory region of the *mabA-inhA* operon (16).

Mutations in *kasA*, which encodes β-ketoacyl ACP synthase (11), and *ndh*, which encodes NADH dehydrogenase (12), have been found in a small proportion of clinical isolates, and we plan to modify our sequencing method to analyze *ndh* and *kasA*.

Our method was sufficient for diagnosis of EMB-resistant isolates, although a limited portion (80%) of *embB* was sequenced. EMB inhibits polymerization of cell wall arabinan of arabinogalactan and of lipoarabinomannan (39). Three homologues of arabinosyltransferases, EmbC, EmbA, and EmbB, have been proposed to be the targets of EMB (32, 39). Mutations in *embB* are found in 47% to 69% of EMB-resistant isolates of *M. tuberculosis* (28, 32). Most EMB-resistant isolates with *embB* mutations exhibited high-level resistance (2, 27). The 35% of EMB-resistant isolates that do not have *embB* mutations showed decreased resistance to EMB (2). We were able to detect a majority (15/18 isolates) of EMB-resistant isolates with our sequencing-based analysis. In addition, we identified two novel mutations, D354A and N296Y, in EMB-resistant isolates in the present study.

pncA is known to be associated with PZA resistance (17, 39). In the present study, we sequenced the complete open reading frame of *pncA* and its promoter region. PZA enters the organism through passive diffusion and is converted to pyrazinoic acid by cytoplasmic PZase. Despite recent progress, the targets of pyrazinoic acid are still not known (39). All PZA-resistant *M. tuberculosis* isolates tested in the present study contained at least one mutation within *pncA* and showed no PZase activity (Table 4). Our results are consistent with those of previous studies that showed 72% to 95% of PZA-resistant clinical isolates of *M. tuberculosis* carried *pncA* mutations (25). All of the *pncA* mutations identified in the present study of PZA-resistant isolates caused amino acid substitutions. Among these mutations, 5A3E, D53N, P54L, C72W, and M175V were novel. The *pncA* mutations were highly diverse and scattered across the gene.

STR, an aminoglycoside, inhibits initiation of mRNA translation. The site of action is the small 30S subunit of the ribosome, especially ribosomal protein S12 and the 16S rRNA (17). *M. tuberculosis* becomes resistant when targets of STR in the ribosomes are mutated. The principal site of mutation is the *rpsL* gene, which encodes ribosomal protein S12 (6, 19, 27). The most frequently observed mutation in *rpsL* was K43R. In the present study, 13 of 30 STR-resistant isolates tested had the K43R mutation. Mutation of the *rrs* gene is also associated with STR resistance in *M. tuberculosis*. *M. tuberculosis* has only a single copy of the *rrs* gene, which encodes the 16S rRNA. Thus, the loops of 16S rRNA that interact with the S12 protein constitute an easily selected mutation site. Such *rrs* mutations are clustered in the highly conserved 530 loop and in the adjacent 915 region (6). In addition, a 1400A→G mutation of *rrs* was identified in both amikacin- and kanamycin-resistant clinical isolates of *M. tuberculosis* (1, 29). These isolates were resistant to STR, indicating that this mutation may contribute to STR resistance (1, 29). In the present study, one STR-resistant isolate had two mutations, 1400A→G and 1539A→G. Because the STR resistance of the isolate can be explained by the 1400A→G mutation, it is unclear whether the 1539A→G mutation is associated with STR resistance.

FQs are active in vitro against *M. tuberculosis* isolates (5) and are increasingly being used in combination with other agents to treat tuberculosis. The principal mechanism of resistance to FQs identified in other bacterial species is alteration of the target proteins DNA gyrase and topoisomerase IV. DNA gyrase is composed of two A and two B subunits, which are encoded by *gyrA* and *gyrB*, respectively (39). Mutations in *gyrA* are associated with high-level resistance of *M. tuberculosis* to FQs (39). *gyrB* mutations associated with resistance have only been identified in laboratory mutants of *M. tuberculosis* (39). Mutations associated with FQ resistance occur within a relatively restricted region of *gyrA*. We identified three mutations, A90V, D94GA, and D94G, in FQ-resistant isolates. We also identified a polymorphism, S95T, that is not associated with FQ resistance. The G88C, D89G, S91P, and D94A, -N, -H, or -Y mutations in *gyrA* have also been found in FQ-resistant isolates (4, 30). These mutations are presumed to be located in the FQ-binding region (4, 30).

Some researchers have described mutations that caused amino acid substitutions but not drug resistance (30, 33, 39). In the present study, we identified several novel mutations that cause amino acid substitutions but do not confer drug resistance. Except for these mutations and silent mutations, the drug resistance profiles of the isolates tested correlated quite

well with the various mutations that we identified (Table 6). The sensitivities of the DNA sequencing-based method (i.e., the ability to detect true drug resistance) were 100%, 89.5%, 83.3%, 100%, 60%, and 100% for the RIF-, INH-, EMB-, PZA-, STR-, and OFX-resistant strains, respectively. The specificities (i.e., the ability to detect true drug susceptibility) were 100% for all drugs tested. The test efficiencies (i.e., the ability to give the correct answer in all samples tested) were 100%, 97.1%, 97.8%, 100%, 91.3%, and 100% for the RIF-, INH-, EMB-, PZA-, STR-, and OFX-resistant strains, respectively. These results indicate that our DNA sequencing-based method is effective for detection of MDR strains. However, when novel mutations in drug resistance-related genes are detected by our method, it is essential to also perform drug susceptibility testing, because novel mutations are not necessarily associated with drug resistance. Of the 25 novel mutations we detected, we cloned 7 novel mutations in KatG. Significant information could be gained if all novel mutations were cloned. For practical purposes, it would be helpful to know the phenotypic manifestations of specific mutations.

In conclusion, we have shown the usefulness of our DNA sequencing strategy for drug susceptibility screening of various targets. Most MDR *M. tuberculosis* strains, which are defined as those strains resistant to both RIF and INH, are resistant to other antitubercular drugs. Our new sequencing-based method can rapidly and efficiently assess MDR of *M. tuberculosis*. The method can also be used to detect MDR *M. tuberculosis* in sputa from patients. Further studies will focus on the clinical application of this method for diagnosis of drug-resistant *M. tuberculosis*.

ACKNOWLEDGMENTS

We thank M. Nakano (Jichi Medical School, Saitama, Japan) for comments on the manuscript, B. L. Triggs-Raine (University of Manitoba, Winnipeg, Canada) for providing *katG*-deficient *E. coli* UM262, and A. S. Swierzko (Centre for Microbiology and Virology, Polish Academy of Sciences, Warsaw, Poland) for coordinating the international collaborative study.

This study was supported by Health Sciences Research grants from the Ministry of Health Labor and Welfare of Japan (H15-SHINKO-3 and H18-SHINKO-IPPAN-012).

REFERENCES

1. **Alangaden, G. J., B. N. Kreiswirth, A. Aouad, M. Khetarpal, F. R. Igno, S. L. Moghazeh, E. K. Manavathu, and S. A. Lerner.** 1998. Mechanism of resistance to amikacin and kanamycin in *Mycobacterium tuberculosis*. Antimicrob. Agents Chemother. **42:**1295–1297.
2. **Alcaide, F., G. E. Pfyffer, and A. Telenti.** 1997. Role of *embB* in natural and acquired resistance to ethambutol in mycobacteria. Antimicrob. Agents Chemother. **41:**2270–2273.
3. **Banerjee, A., M. Sugantino, J. C. Sacchettini, and W. R. Jacobs, Jr.** 1998. The *mabA* gene from the *inhA* operon of *Mycobacterium tuberculosis* encodes a 3-ketoacyl reductase that fails to confer isoniazid resistance. Microbiology **144:**2697–2704.
4. **Barnard, F. M., and A. Maxwell.** 2001. Interaction between DNA gyrase and quinolones: effects of alanine mutations at GyrA subunit residues Ser^{83} and Asp^{87}. Antimicrob. Agents Chemother. **45:**1994–2000.
5. **Chen, C. H., J. F. Shih, P. J. Lindholm-Levy, and L. B. Heifets.** 1989. Minimal inhibitory concentrations of rifabutin, ciprofloxacin, and ofloxacin against *Mycobacterium tuberculosis* isolated before treatment of patients in Taiwan. Am. Rev. Respir. Dis. **140:**987–989.
6. **Finken, M., P. Kirschner, A. Meier, A. Wrede, and E. C. Bottger.** 1993. Molecular basis of streptomycin resistance in *Mycobacterium tuberculosis*: alterations of the ribosomal protein S12 gene and point mutations within a functional 16S ribosomal RNA pseudoknot. Mol. Microbiol. **9:**1239–1246.
7. **Fluit, A. C., M. R. Visser, and F.-J. Schmitz.** 2001. Molecular detection of antimicrobial resistance. Clin. Microbiol. Rev. **14:**836–871.
8. **Garnier, T., K. Eiglmeier, J. C. Camus, N. Medina, H. Mansoor, M. Pryor, S. Duthoy, S. Grondin, C. Lacroix, C. Monsempe, S. Simon, B. Harris, R. Atkin, J. Doggett, R. Mayes, L. Keating, P. R. Wheeler, J. Parkhill, B. G. Barrell, S. T. Cole, S. V. Gordon, and R. G. Hewinson.** 2003. The complete genome sequence of *Mycobacterium bovis*. Proc. Natl. Acad. Sci. USA **100:**7877–7882.
9. **Heym, B., P. M. Alzari, N. Honore, and S. T. Cole.** 1995. Missense mutations in the catalase-peroxidase gene, katG, are associated with isoniazid resistance in *Mycobacterium tuberculosis*. Mol. Microbiol. **15:**235–245.
10. **Lavender, C., M. Globan, A. Sievers, H. Billman-Jacobe, and J. Fyfe.** 2005. Molecular characterization of isoniazid-resistant *Mycobacterium tuberculosis* isolates collected in Australia. Antimicrob. Agents Chemother. **49:**4068–4074.
11. **Lee, A. S. G., I. H. K. Lim, L. L. H. Tang, A. Telenti, and S. Y. Wong.** 1999. Contribution of *kasA* analysis to detection of isoniazid-resistant *Mycobacterium tuberculosis* in Singapore. Antimicrob. Agents Chemother. **43:**2087–2089.
12. **Lee, A. S. G., A. S. M. Teo, and S.-Y. Wong.** 2001. Novel mutations in *ndh* in isoniazid-resistant *Mycobacterium tuberculosis* isolates. Antimicrob. Agents Chemother. **45:**2157–2159.
13. **Loewen, P. C., J. Switala, M. Smolenski, and B. L. Triggs-Raine.** 1990. Molecular characterization of three mutations in *katG* affecting the activity of hydroperoxidase I of *Escherichia coli*. Biochem. Cell Biol. **68:**1037–1044.
14. **Miller, L. P., J. T. Crawford, and T. M. Shinnick.** 1994. The *rpoB* gene of *Mycobacterium tuberculosis*. Antimicrob. Agents Chemother. **38:**805–811.
15. **Miller, M. A., L. Thibert, F. Desjardins, S. H. Siddiqi, and A. Dascal.** 1995. Testing of susceptibility of *Mycobacterium tuberculosis* to pyrazinamide: comparison of Bactec method with pyrazinamidase assay. J. Clin. Microbiol. **33:**2468–2470.
16. **Morris, S., G. H. Bai, P. Suffys, L. Portillo-Gomez, M. Fairchok, and D. Rouse.** 1995. Molecular mechanisms of multiple drug resistance in clinical isolates of *Mycobacterium tuberculosis*. J. Infect. Dis. **171:**954–960.
17. **Musser, J. M.** 1995. Antimicrobial agent resistance in mycobacteria: molecular genetic insights. Clin. Microbiol. Rev. **8:**496–514.
18. **Nagy, J. M., A. E. Cass, and K. A. Brown.** 1997. Purification and characterization of recombinant catalase-peroxidase, which confers isoniazid sensitivity in *Mycobacterium tuberculosis*. J. Biol. Chem. **272:**31265–31271.
19. **Nair, J., D. A. Rouse, G. H. Bai, and S. L. Morris.** 1993. The *rpsL* gene and streptomycin resistance in single and multiple drug-resistant strains of *Mycobacterium tuberculosis*. Mol. Microbiol. **10:**521–527.
20. **National Committee for Clinical Laboratory Standards.** 2000. Susceptibility testing of mycobacteria, nocardia, and other aerobic actinomycetes. Tentative standard M24-T2, 2nd ed. National Committee for Clinical Laboratory Standards, Wayne, Pa.
21. **Otsuka, Y., P. Parniewski, Z. Zwolska, M. Kai, T. Fujino, F. Kirikae, E. Toyota, K. Kudo, T. Kuratsuji, and T. Kirikae.** 2004. Characterization of a trinucleotide repeat sequence $(CGG)_5$ and potential use in restriction fragment length polymorphism typing of *Mycobacterium tuberculosis*. J. Clin. Microbiol. **42:**3538–3548.
22. **Ramaswamy, S. V., R. Reich, S.-J. Dou, L. Jasperse, X. Pan, A. Wanger, T. Quitugua, and E. A. Graviss.** 2003. Single nucleotide polymorphisms in genes associated with isoniazid resistance in *Mycobacterium tuberculosis*. Antimicrob. Agents Chemother. **47:**1241–1250.
23. **Roberts, G. D., N. L. Goodman, L. Heifets, H. W. Larsh, T. H. Lindner, J. K. McClatchy, M. R. McGinnis, S. H. Siddiqi, and P. Wright.** 1983. Evaluation of the BACTEC radiometric method for recovery of mycobacteria and drug susceptibility testing of *Mycobacterium tuberculosis* from acid-fast smear-positive specimens. J. Clin. Microbiol. **18:**689–696.
24. **Rouse, D. A., J. A. DeVito, Z. Li, H. Byer, and S. L. Morris.** 1996. Site-directed mutagenesis of the *katG* gene of *Mycobacterium tuberculosis*: effects on catalase-peroxidase activities and isoniazid resistance. Mol. Microbiol. **22:**583–592.
25. **Scorpio, A., P. Lindholm-Levy, L. Heifets, R. Gilman, S. Siddiqi, M. Cynamon, and Y. Zhang.** 1997. Characterization of *pncA* mutations in pyrazinamide-resistant *Mycobacterium tuberculosis*. Antimicrob. Agents Chemother. **41:**540–543.
26. **Scorpio, A., and Y. Zhang.** 1996. Mutations in *pncA*, a gene encoding pyrazinamidase/nicotinamidase, cause resistance to the antituberculous drug pyrazinamide in tubercle bacillus. Nat. Med. **2:**662–667.
27. **Sreevatsan, S., X. Pan, K. E. Stockbauer, D. L. Williams, B. N. Kreiswirth, and J. M. Musser.** 1996. Characterization of *rpsL* and *rrs* mutations in streptomycin-resistant *Mycobacterium tuberculosis* isolates from diverse geographic localities. Antimicrob. Agents Chemother. **40:**1024–1026.
28. **Sreevatsan, S., K. E. Stockbauer, X. Pan, B. N. Kreiswirth, S. L. Moghazeh, W. R. Jacobs, Jr., A. Telenti, and J. M. Musser.** 1997. Ethambutol resistance in *Mycobacterium tuberculosis*: critical role of *embB* mutations. Antimicrob. Agents Chemother. **41:**1677–1681.
29. **Suzuki, Y., C. Katsukawa, A. Tamaru, C. Abe, M. Makino, Y. Mizuguchi, and H. Taniguchi.** 1998. Detection of kanamycin-resistant *Mycobacterium tuberculosis* by identifying mutations in the 16S rRNA gene. J. Clin. Microbiol. **36:**1220–1225.
30. **Takiff, H. E., L. Salazar, C. Guerrero, W. Philipp, W. M. Huang, B. Kreiswirth, S. T. Cole, W. R. Jacobs, Jr., and A. Telenti.** 1994. Cloning and

nucleotide sequence of *Mycobacterium tuberculosis gyrA* and *gyrB* genes and detection of quinolone resistance mutations. Antimicrob. Agents Chemother. **38:**773–780.

31. **Telenti, A., P. Imboden, F. Marchesi, D. Lowrie, S. Cole, M. J. Colston, L. Matter, K. Schopfer, and T. Bodmer.** 1993. Detection of rifampicin-resistance mutations in *Mycobacterium tuberculosis*. Lancet **341:**647–650.
32. **Telenti, A., W. J. Philipp, S. Sreevatsan, C. Bernasconi, K. E. Stockbauer, B. Wieles, J. M. Musser, and W. R. Jacobs, Jr.** 1997. The *emb* operon, a gene cluster of *Mycobacterium tuberculosis* involved in resistance to ethambutol. Nat. Med. **3:**567–570.
33. **van Doorn, H. R., E. J. Kuijper, A. van der Ende, A. G. A. Welten, D. van Soolingen, P. E. W. de Haas, and J. Dankert.** 2001. The susceptibility of *Mycobacterium tuberculosis* to isoniazid and the Arg→Leu mutation at codon 463 of *katG* are not associated. J. Clin. Microbiol. **39:**1591–1594.
34. **Wayne, L. G.** 1974. Simple pyrazinamidase and urease tests for routine identification of mycobacteria. Am. Rev. Respir. Dis. **109:**147–151.
35. **Wei, C.-J., B. Lei, J. M. Musser, and S.-C. Tu.** 2003. Isoniazid activation defects in recombinant *Mycobacterium tuberculosis* catalase-peroxidase (KatG) mutants evident in InhA inhibitor production. Antimicrob. Agents Chemother. **47:**670–675.
36. **Yu, S., S. Chouchane, and R. S. Magliozzo.** 2002. Characterization of the W321F mutant of *Mycobacterium tuberculosis* catalase-peroxidase KatG. Protein Sci. **11:**58–64.
37. **Yu, S., S. Girotto, X. Zhao, and R. S. Magliozzo.** 2003. Rapid formation of compound II and a tyrosyl radical in the Y229F mutant of *Mycobacterium tuberculosis* catalase-peroxidase disrupts catalase but not peroxidase function. J. Biol. Chem. **278:**44121–44127.
38. **Zhang, Y., B. Heym, B. Allen, D. Young, and S. Cole.** 1992. The catalase-peroxidase gene and isoniazid resistance of *Mycobacterium tuberculosis*. Nature **358:**591–593.
39. **Zhang, Y., and A. Telenti.** 2000. Genetics of drug resistance in *Mycobacterium tuberculosis*, p. 235–254. *In* G. F. Hatfull and W. R. Jabobs (ed.), Molecular genetics of mycobacteria. American Society for Microbiology, Washington, DC.
40. **Zumia, A., and J. M. Grange.** 2001. Multidrug-resistant tuberculosis—can the tide be turned? Lancet Infect. Dis. **1:**199–202.

FtsZ: A Novel Target for Tuberculosis Drug Discovery

Qing Huang[1], Peter J. Tonge[1,2], Richard A. Slayden[3], Teruo Kirikae[4] and Iwao Ojima[1,2,*]

[1]*Department of Chemistry, State University of New York at Stony Brook, Stony Brook, New York 11794-3400, USA,* [2]*Institute of Chemical Biology & Drug Discovery, The Chemistry Bldg., State University of New York at Stony Brook, New York 11794-3400, USA,* [3]*Department of Microbiology, Immunology and Pathology, Colorado State University, Fort Collins, Colorado 80523-1682, USA,* [4]*Department of Infectious Diseases, Research Institute, International Medical Center of Japan, 1-21-1, Toyama, Shinjuku, Tokyo, 162-8655, Japan*

Abstract: The emergence of multi-drug resistant *Mycobacterium tuberculosis* (Mtb) strains has made many of the currently available anti-TB drugs ineffective. Accordingly there is a pressing need to identify new drug targets. FtsZ, a bacterial tubulin homologue, is an essential cell division protein that polymerizes in a GTP-dependent manner, forming a highly dynamic cytokinetic ring, designated as the Z ring, at the septum site. Following recruitment of other cell division proteins, the Z ring contracts, resulting in closure of the septum and then formation of two daughter cells. Since inactivation of FtsZ or alteration of FtsZ assembly results in the inhibition of Z ring and septum formation, FtsZ is a very promising target for new antimicrobial drug development. This review describes the function and dynamic behaviors of FtsZ, its homology to tubulin, and recent development of FtsZ inhibitors as potential anti-TB agents.

Keywords: FtsZ, tubulin, GTPase, homology, GTP hydrolysis, polymerization, dynamics, inhibitor.

INTRODUCTION

Global TB Problems and the Need for New TB Drugs

Tuberculosis (TB) was one of the first infectious diseases identified. It was thought by many that it could be eradicated, but the disease has re-emerged [1] and is today the leading cause of death in the world from a single infectious disease [2]. TB and HIV/AIDS form a lethal combination, each speeding the other's progress. This coinfection has become increasingly common. We can't effectively fight HIV/AIDS without also fighting TB. Recent statistics from WHO estimate that there are about 8.4 million new cases every year [3] with a global mortality rate of 23 % [2, 4-6].

Poor chemotherapeutics and inadequate local-control programs contribute to the inability to manage TB and lead to the emergence of drug resistant strains of Mtb [4]. Treating drug-resistant TB is much more difficult, which takes 18 to 24 months if the patient responds to the second-line treatment regimen and is around 20 times more expensive than treating fully drug sensitive TB. The currently available second-line drugs are less effective, and have more side-effects [7], thus, warranting the identification of novel drug targets and development of new chemotherapeutics.

In eukaryotic pathogens, as well as in higher eukaryotic cells, cell division has been a productive area for finding drugs that combat infection or uncontrolled cell proliferation [8-10], while the bacterial cell division machinery has remained largely unexploited for therapeutic purposes [11]. Recently, FtsZ, a tubulin homologue involved in bacterial cell division, has received considerable attention and has been considered as an attractive target to develop novel anti-TB drugs, as well as new broad-spectrum antibacterial agents.

*Address correspondence to this author at Department of Chemistry, State University of New York at Stony Brook, Stony Brook, New York 11794-3400, USA; Tel: (631) 632-7890; Fax: (631) 632-7942; E-mail: iojima@notes.cc.sunysb.edu

FILAMENT-FORMING TEMPERATURE-SENSITIVE GENE Z (FtsZ)

The Role of FtsZ in Bacterial Cytokinesis

In the 1960s, genes designated "Fts" (filament-forming temperature-sensitive genes, *fts*), were identified by mutational analysis in *Escherichia coli*. The gene products of the Fts-genes are known to be involved in septum formation [12, 13]. While the involvement of Fts-proteins in cell division was known, it was not discovered until 1991 that FtsZ was involved in Z ring formation and the initiation of cell division [14].

FtsZ is the most abundant cell division protein and plays an essential role in bacteria cytokinesis. In the presence of GTP, FtsZ polymerization is initiated at a single site on the inner membrane at mid-cell and appears to grow bidirectionally to form a highly dynamic helical structure [15-18], designated as the Z-ring, that encircles the cell [19]. Following recruitment of the other cell division proteins, the Z-ring contracts, resulting in septum formation [20] (Fig. **1**). Assembly of FtsZ is regulated by FtsZ interacting proteins, which include stabilizing factors, such as ZapA, ZipA and FtsA, as well as destabilizing factors, such as SulA, EzrA and MinCD [15]. Hence, the stability of FtsZ is precisely tuned. Inactivation of FtsZ results in a complete absence of septum formation. Accordingly, FtsZ is a very promising target for new anti-microbial drug discovery because of its central role in cell division and its known biochemical activity. This is a novel drug target and thus new agents targeting FtsZ would not be affected by known drug-resistance mechanisms caused by the use of current anti-TB drugs.

1568-0266/07 $50.00+.00

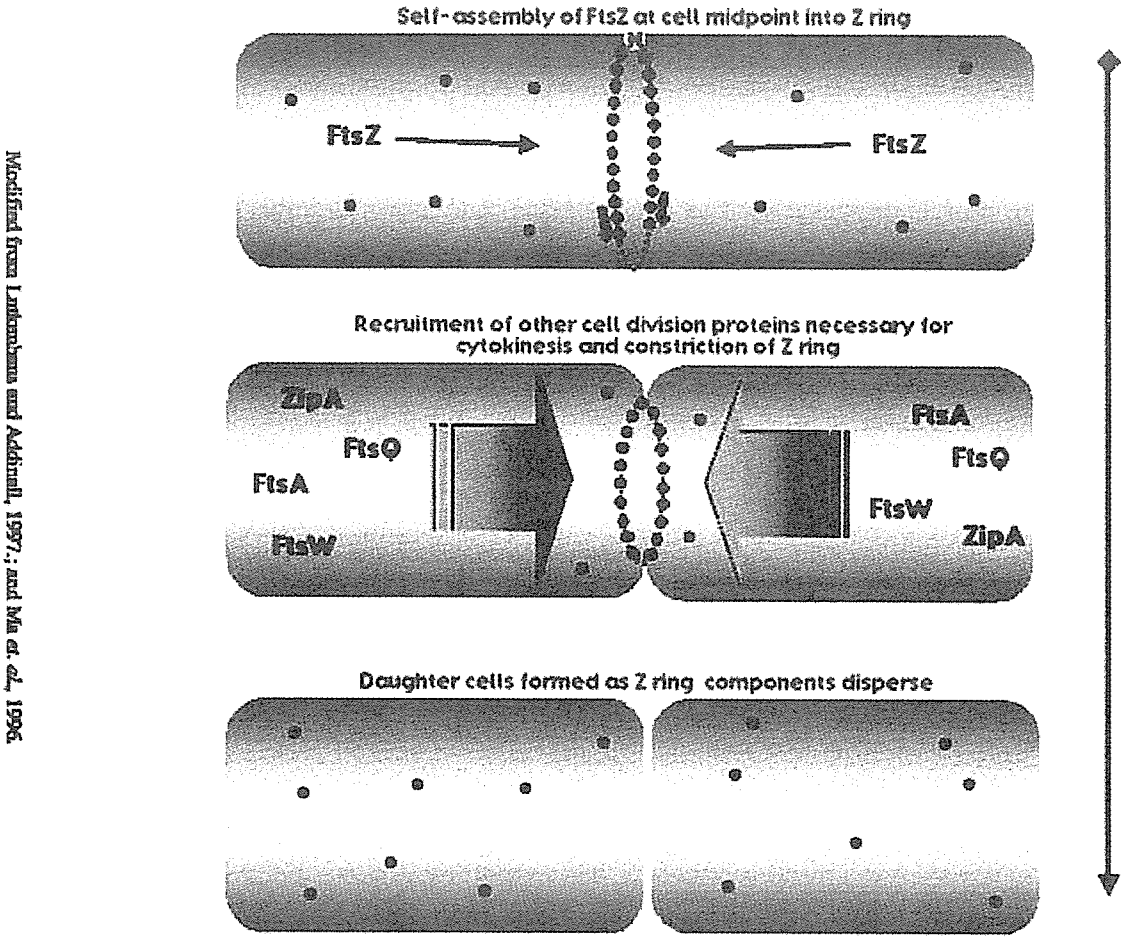

Fig. (1). Diagram of cell division and the Z-ring.
Figure adapted from http://www.umass.edu/microbio/ with permission from Drs. Gabriel McCool and Maura C. Cannon.

FtsZ Dynamics: GTP Hydrolysis and FtsZ Polymerization

Experiments measuring FtsZ-GFP fluorescence recovery after photobleaching (FRAP) have revealed that the Z ring is extremely dynamic, continuously remodeling itself before and during constriction with a rate comparable to that of microtubules [19]. The amount of FtsZ in *E. Coli* has been estimated to be about 15,000 molecules / cell [21], but only one third of the cellular FtsZ pool is present in the ring at a given time [22]. FtsZ subunits exchange in and out of the ring on a time scale of seconds even when the overall morphology of the ring appears static [23]. The highly dynamic nature of the Z ring is due to FtsZ's capacity for GTP-dependent, reversible polymerization [24]. The constant balance between assembly and disassembly means that small changes in FtsZ polymerization dynamics are able to trigger large and rapid changes in FtsZ's structure in the cell [24]. Understanding FtsZ polymer dynamics will aid the development of drugs that can prevent cell division by disrupting Z ring formation.

The relation between FtsZ polymerization and GTP hydrolysis has been a subject of numerous studies [24-36]. The clear link between GTP hydrolysis and polymerization dynamics was first shown when the formation of FtsZ polymers in solution was found to be coupled with GTP hydrolysis, i.e., polymer loss coincided with GTP depletion [37, 38]. Recently, Romberg and Timothy [33] investigated GTP hydrolysis in FtsZ polymers using several complementary approaches that avoided the technical caveats of previous studies, and proposed a model for the FtsZ hydrolysis cycle (Fig. **2**). GTP-FtsZ polymerizes into straight polymers, first. The association of FtsZ monomers triggers the GTPase activity of FtsZ [31], since the catalytic site is formed at the interface of two adjacent FtsZs. The GTP-binding domain is located on one monomer and the highly conserved tubulin-like loop 7 (T7-loop) of the other domain is located on an adjacent FtsZ monomer (Fig. **3**). It is thought that GTP hydrolysis induces a structural change at the nucleotide-protein interface by pushing against the T7-loop region of the adjacent monomer. The binding geometry can be used to rationalize why GTP binding promotes polymerization of FtsZ and why GTP hydrolysis is associated with FtsZ depolymerization [23]. During steady-state GTP turnover, the properties of the polymer will be determined by the nucleotide species that predominates. In turn, the predominant nucleotide species will be determined by the rate-limiting step in FtsZ's hydrolysis cycle [33]. Results from pre-steady-state single turnover assays indicate that GTP hydrolysis is the major rate-limiting step ($k_{\text{hydrolysis}}$

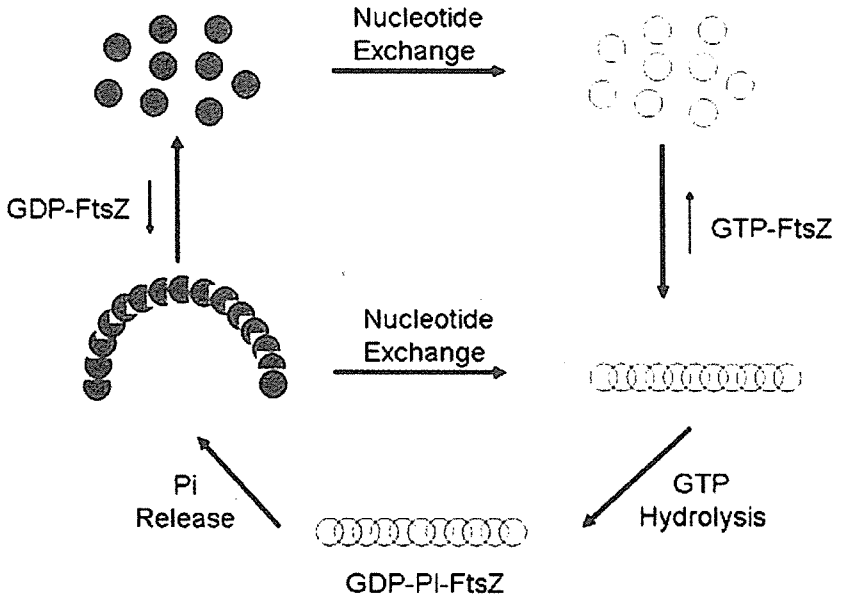

Fig. (2). Model of FtsZ hydrolysis circle. FtsZ's hydrolysis cycle is coupled to polymer assembly and disassembly. Reprinted from [24], with permission from the Annual Review of Microbiology, Volume 57 ©2003 by Annual Reviews, www.annualreviews.org.

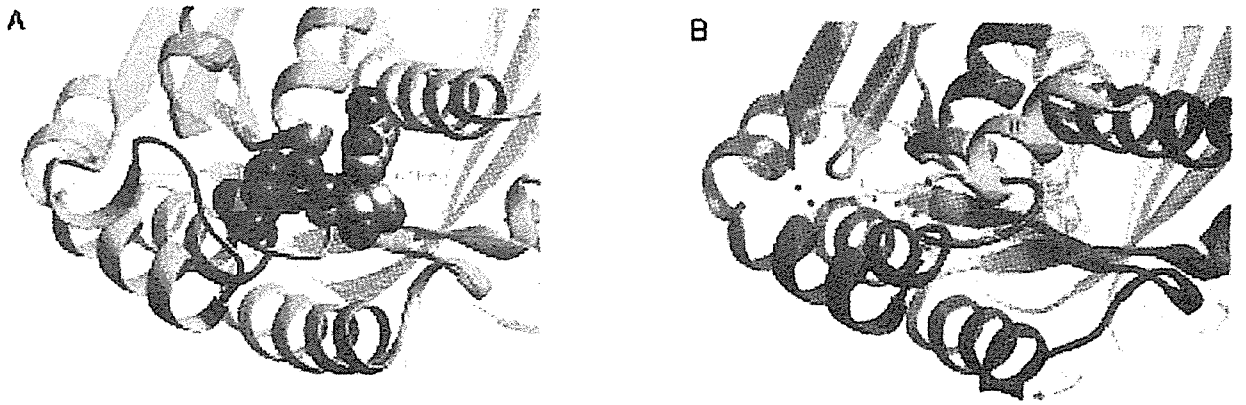

Fig. (3). The conformational switch. The region between β2 and β3 adopts two distinct conformations in Mtb FtsZ. The ordered T3 loop ("Switch II") in subunit A is apposed to the γ-thiophosphate of GTPγS and to the sH2 switch α-helix ("Switch I"). In subunit B, T3 is disordered (balls), and the switch has "switched" to the sβ2 β-strand conformation. Reprinted from [16] *J. Mol. Biol*., *342*, (3). Leung, A. K. W.; White, E. L.; Ross, L. J.; Reynolds, R. C.; DeVito, J. A.; Borhani, D. W.. Structure of Mycobacterium tuberculosis FtsZ Reveals Unexpected, G Protein-like Conformational Switches. 953-970., Copyright (2004), with permission from Elsevier.

≈ 8/min) and phosphate release rapidly follows ($k_{Pi\ release}$ >> 8/min). At steady state, 80% of FtsZ polymer subunits are bound to GTP [33], and FtsZ undergoes facile GDP exchange with free GTP in solution [39, 40]. Polymer stability is directly affected by the rate of GTP hydrolysis, since FtsZ-GTP is stable, whereas FtsZ-GDP is the form that favors depolymerization [24]. With the energy provided by GTP hydrolysis, polymers bound to GDP tend to curve and become more labile, which leads to constriction of the Z ring in cell division [33]. The step leading to GDP release from the polymer might be partially rate limiting. GDP release may occur either by direct nucleotide exchange in the polymers [29, 33, 39-42] or via depolymerization and subsequent nucleotide exchange in the monomers [33, 42].

Based on the structure of Mtb FtsZ, Leung *et al.*[16] identified subunit interactions in FtsZ analogous to the two conformational switches that are critical to G protein function (Fig. **3**) and that link GTP binding and hydrolysis to FtsZ lateral assembly and Z-ring contraction. Mtb FtsZ Switch I region, i.e. sH2 (switch helix2, residues 41-50) is located in the GTPase domain, and forms much of the dimer interface. The presence of a γ- (thio) phosphate from the GTP analogue GTPγS in the FtsZ active site, causes an ordering and closing inwards of "tubulin" loop T3, which is designated as the Switch II region of Mtb FtsZ. The ordering of T3 will force Switch I to adopt the sH2 conformation to avoid spatial overlap, while disordering of T3 upon GTP hydrolysis will alter the intersubunit A/B packing by enabling the sH2-to-sβ2 structural transition at the lateral